

Journal of Visualized Experiments

Theoretical Calculation and Experimental Verification for Dislocation Reduction in Germanium Epitaxial Layers with Semicylindrical Voids on Silicon --Manuscript Draft--

Article Type:	Invited Methods Article - JoVE Produced Video
Manuscript Number:	JoVE58897R3
Full Title:	Theoretical Calculation and Experimental Verification for Dislocation Reduction in Germanium Epitaxial Layers with Semicylindrical Voids on Silicon
Keywords:	Germanium; silicon; Photonics; Integrated Photonics; Devices; materials; Systems
Corresponding Author:	Kazumi Wada Massachusetts Institute of Technology Cambridge, MA UNITED STATES
Corresponding Author's Institution:	Massachusetts Institute of Technology
Corresponding Author E-Mail:	kwada@mit.edu
Order of Authors:	Kazumi Wada Motoki Yako Yasuhiko Ishikawa Eiji Abe
Additional Information:	
Question	Response
Please indicate whether this article will be Standard Access or Open Access.	Standard Access (US\$2,400)
Please indicate the city, state/province, and country where this article will be filmed. Please do not use abbreviations.	Toyohashi, Japan and Cambridge, MA

Letter to the Editor

Title: Theoretical Calculation and Experimental Verification for Dislocation Reduction in Ge Epitaxial Layers with Semicylindrical Voids on Si

Submission number: JoVE58897

Dear Dr. Vineeta Bajaj,
Review Editor of JoVE,

We are grateful to submit our manuscript to JoVE, originally entitled “A method of dislocation reduction in Ge epitaxial layers with semicylindrical voids on Si: theoretical calculation and experimental verification,” and revised to “Theoretical Calculation and Experimental Verification for Dislocation Reduction in Ge Epitaxial Layers with Semicylindrical Voids on Si.”

We have revised our manuscript in response to the editorial comments, and prepared a manuscript for review. Important changes and added descriptions are highlighted by **RED** color in the revised manuscript for review.

[Comments]

Changes to be made by the author(s) regarding the manuscript:

1. Please take this opportunity to thoroughly proofread the manuscript to ensure that there are no spelling or grammar issues.
2. Please revise lines 308-310 to avoid previously published text.

[Reply]

We have revised the lines 308–310 (lines 366–368 in the revised manuscript) to avoid previously published text. Thank you for the comment.

[Comment]

3. Please obtain explicit copyright permission to reuse any figures from a previous publication. Explicit permission can be expressed in the form of a letter from the editor or a link to the editorial policy that allows re-prints. Please upload this information as a .doc or .docx file to your Editorial Manager account. The Figure must be cited appropriately in the Figure Legend, i.e. “This figure has been modified from [citation].”

[Reply]

We have revised the figure captions, and uploaded the information of copyright permission for the reuse of figures from a previous publication [20] in the revised manuscript.

[20] Yako, M., Ishikawa, Y., Abe, E., Wada, K., Defects and Their Reduction in Ge Selective Epitaxy and Coalescence Layer on Si With Semicylindrical Voids on SiO₂ Masks, *IEEE Journal of Selected Topics in Quantum Electronics*, 24 (6), 8201007 (2018).

[Comments]

4. Please ensure that the figures are properly labeled and match their corresponding

figure legends. See some inconsistencies listed below.

5. Figure 3: The uploaded Figure 3 does not match the description in figure legend. Please revise.

6. Figure 4: The uploaded Figure 4 seems to match figure legend of Figure 3.

7. Figures 6 and 8: Please use “°C” for the temperature unit and include a space between numbers and their units (700 °C, etc.).

8. Figure 11: Please describe what the green and red ellipses stand for.

9. What is the difference between Figure 2 and Figure 2R? Please upload only one Figure 2.

10. Please reference Figure 2 and Figure 7 in the manuscript. Please number the figures in the sequence in which you refer to them in the manuscript text.

[Reply]

For Figs. 3 and 4 (Figs. 4 and 5 in the revised manuscript): we have checked the figure labels and now they are correctly labeled.

Figures 6 and 8 (Figs. 7 and 9 in the revised manuscript) are revised to use “°C” and include a space between numbers and their units.

We have added descriptions for green and red ellipses in Fig. 11 (Fig. 12 in the revised manuscript) in the revised manuscript (lines 489–493, highlighted by RED color).

We are afraid there were some mistakes in uploading the figures/movies in the last submission. We believe they are submitted correctly and there is no “Figure 2R” this time.

In the revised manuscript, Fig. 2 is referred in “PROTOCOL” part (lines 110, 114, and 118), and Fig. 7 (Fig. 8 in the revised manuscript) is referred in “REPRESENTATIVE RESULTS” part (from line 341). Please find the RED colored text showing where they are referred.

[Comment]

11. Table of Materials: Please revise to include the name, company, and catalog number of all relevant supplies, reagents, equipment and software in separate columns in an xls/xlsx file. Please sort the items in alphabetical order according to the name of material/equipment.

[Reply]

We have revised the Table of Materials to include the detailed information of the material/equipment used in the experiments.

[Comments]

12. Please revise the title to avoid the use of colon.

[Reply]

We have revised the title as

“Theoretical Calculation and Experimental Verification for Dislocation Reduction in Ge Epitaxial Layers with Semicylindrical Voids on Si”

to avoid the use of colon.

[Comment]

13. Please revise the protocol text to avoid the use of any personal pronouns (e.g., "we", "you", "our" etc.).

[Reply]

We have revised the PROTOCOL part and removed all personal pronouns from the revised manuscript.

[Comments]

14. Please add more details to your protocol steps. There should be enough detail in each step to supplement the actions seen in the video so that viewers can easily replicate the protocol. Please ensure you answer the “how” question, i.e., how is the step performed? Alternatively, add references to published material specifying how to perform the protocol action. See examples below.

15. 2.1.1: Please specify the mass/size of the substrates used.

16. 2.1.2: Please describe how electron beam (EB) lithography and wet etching are done.

17. 2.1.3: How to set different parameters?

18. 2.1.4: Please describe how to prepare square-shaped Si window areas of 4 mm in width. What parameters are set differently?

19. 2.1.5: Do the Si wafers refer to product from 2.1.3 or 2.1.4 or both? Please specify the concentration of HF used.

20. 2.2.1-2.2.5: Please reorganize these steps so that they can be followed in chronological order.

21. 2.2.5: Please describe how to perform periodic insertion of 10-nm-thick Si_{0.3}Ge_{0.7} demarcation layers.

22. 2.3.2: Please describe how this is done.

[Reply]

We have added more details in protocol steps.

Answer for each question:

15: 4 inch Si substrates were used (section 2.1.4 in the revised manuscript).

16: more details in EB lithography (sections 2.1.6–2.1.10) and wet etching (sections 2.1.11–2.1.13) have been described in the revised manuscript.

17 and 18: the SEG mask design was determined by creating design file. We have added description about creating the design file (sections 2.1.1–2.1.3) in the revised manuscript.

19: The Si wafers are the same one described in the former sections. In fact, we used both the words “wafer” and “substrate” for the same thing. In the revised manuscript, we use only “substrate”. The concentration of HF for the each step is added in the revised manuscript.

20: We have added more detail of Ge growth protocol in section 2.2.1–2.2.6.

21: 10-nm-thick Si_{0.3}Ge_{0.7} layers were inserted by just introducing Si₂H₆ gas in Ge growth chamber. We have added a description in section 2.2.6.

22. We have added more detailed description about EPD measurements in section 2.3.1–2.3.4.

[Comment]

23. JoVE articles are focused on the methods and the protocol, thus the discussion should be similarly focused. Please revise the Discussion to explicitly cover the following in detail in 3-6 paragraphs with citations:

- a) Critical steps within the protocol
- b) Any modifications and troubleshooting of the technique
- c) Any limitations of the technique
- d) The significance with respect to existing methods
- e) Any future applications of the technique

[Reply]

We have revised the discussion part so as to focus on the points a)–e) above.

a) Critical steps within the protocol are (A) SEG mask preparation and (B) epitaxial Ge growth, as mentioned in lines 560–562 (highlighted by **RED** color).

Then, b) and c) are described for each steps (lines 564–583).

d) is described in lines 585–593 and Table 1, and e) is described in lines 598–601.

[Comment]

24. Please ensure that the references appear as the following: [Lastname, F.I., LastName, F.I., LastName, F.I. Article Title. Source. Volume (Issue), FirstPage – LastPage (YEAR).] For more than 6 authors, list only the first author then et al. Please do not abbreviate journal titles. See the example below:

Bedford, C.D., Harris, R.N., Howd, R.A., Goff, D.A., Koolpe, G.A. Quaternary salts of 2-[(hydroxyimino)methyl]imidazole. Journal of Medicinal Chemistry. 32 (2), 493-503 (1998).

[Reply]

We have revised the form of references as pointed out.

Thank you again for your kind support and consideration on our submission to JoVE.

For the payment: since fiscal year in Japan starts from April, our budget requests us to pay before the end of February.

We would be grateful if you would kindly take into account the situation for the final judgement.

Sincerely,

Motoki Yako

Ph.D. candidate
Department of Materials Engineering
University of Tokyo

TITLE:

Theoretical Calculation and Experimental Verification for Dislocation Reduction in Germanium Epitaxial Layers with Semicylindrical Voids on Silicon

AUTHORS AND AFFILIATIONS:

Motoki Yako¹, Yasuhiko Ishikawa², Eiji Abe¹, Kazumi Wada^{1,3}

¹Department of Materials Engineering, The University of Tokyo, Bunkyo-ku, Tokyo, Japan

²Department of Electrical and Electronic Information Engineering, Toyohashi University of Technology, Toyohashi, Japan

³Department of Materials Science and Engineering, Massachusetts Institute of Technology, Cambridge, MA, USA

Corresponding author:

Kazumi Wada (kwada@mit.edu)

Email addresses of co-authors:

Motoki Yako (yako@emat.t.u-tokyo.ac.jp)

Yasuhiko Ishikawa (ishikawa@ee.tut.ac.jp)

Eiji Abe (abe@material.t.u-toyko.ac.jp)

KEYWORDS:

Silicon photonics, germanium, Ge, crystal growth, selective epitaxial growth, threading dislocation density, image force, theoretical calculation, chemical vapor deposition, CVD, transmission electron microscope, TEM

SUMMARY:

Theoretical calculation and experimental verification are proposed for a reduction of threading dislocation (TD) density in germanium epitaxial layers with semicylindrical voids on silicon. Calculations based on the interaction of TDs and surface via image force, TD measurements, and transmission electron microscope observations of TDs are presented.

ABSTRACT:

Reduction of threading dislocation density (TDD) in epitaxial germanium (Ge) on silicon (Si) has been one of the most important challenges for the realization of monolithically integrated photonics circuits. The present paper describes methods of theoretical calculation and experimental verification of a novel model for the reduction of TDD. The method of theoretical calculation describes the bending of threading dislocations (TDs) based on the interaction of TDs and non-planar growth surfaces of selective epitaxial growth (SEG) in terms of dislocation image force. The calculation reveals that the presence of voids on SiO₂ masks help to reduce TDD. Experimental verification is described by germanium (Ge) SEG, using an ultra-high vacuum chemical vapor deposition method and TD observations of the grown Ge via etching and cross-sectional transmission electron microscope (TEM). It is strongly suggested that the TDD reduction would be due to the presence of semicylindrical voids over the SiO₂ SEG masks and growth

temperature. For experimental verification, epitaxial Ge layers with semicylindrical voids are formed as the result of SEG of Ge layers and their coalescence. The experimentally obtained TDDs reproduce the calculated TDDs based on the theoretical model. Cross-sectional TEM observations reveal that both the termination and generation of TDs occur at semicylindrical voids. Plan-view TEM observations reveal a unique behavior of TDs in Ge with semicylindrical voids (i.e., TDs are bent to be parallel to the SEG masks and the Si substrate).

INTRODUCTION:

Epitaxial Ge on Si has attracted substantial interests as an active photonic device platform since Ge can detect/emit light in the optical communication range (1.3–1.6 μm) and is compatible with Si CMOS (complementary metal oxide semiconductor) processing techniques. However, since the lattice mismatch between Ge and Si is as large as 4.2%, threading dislocations (TDs) are formed in Ge epitaxial layers on Si at a density of $\sim 10^9/\text{cm}^2$. The performances of Ge photonic devices are deteriorated by TDs because TDs works as carrier generation centers in Ge photodetectors (PDs) and modulators (MODs), and as carrier recombination centers in laser diodes (LDs). In turn, they would increase reverse leakage current (J_{leak}) in PDs and MODs^{1–3}, and threshold current (J_{th}) in LDs^{4–6}.

Various attempts have been reported to reduce TD density (TDD) in Ge on Si (**Supplemental Figure 1**). Thermal annealing stimulates movement of TDs leading to the reduction of TDD, typically to $2 \times 10^7/\text{cm}^2$. The drawback is the possible intermixing of Si and Ge and out-diffusion of dopants in Ge such as phosphorus^{7–9} (**Supplemental Figure 1a**). The SiGe graded buffer layer^{10–12} increases the critical thicknesses and suppresses the generation of TDs leading to the reduction of TDD, typically to $2 \times 10^6/\text{cm}^2$. The drawback here is that the thick buffer reduces light coupling efficiency between Ge devices and Si waveguides underneath (**Supplemental Figure 1b**). Aspect ratio trapping (ART)^{13–15} is a selective epitaxial growth (SEG) method and reduces TDs by trapping TDs at the sidewalls of thick SiO_2 trenches, typically to $<1 \times 10^6/\text{cm}^2$. The ART method uses a thick SiO_2 mask to reduce TDD in Ge over the SiO_2 masks, which locates far above Si and have the same drawback (**Supplemental Figure 1b,1c**). Ge growth on Si pillar seeds and annealing^{16–18} are similar to the ART method, enabling TD trapping by the high aspect ratio Ge growth, to $<1 \times 10^5/\text{cm}^2$. However, high temperature annealing for Ge coalescence has the same drawbacks in **Supplemental Figure 1a–c** (**Supplemental Figure 1d**).

To achieve low-TDD Ge epitaxial growth on Si that is free from the drawbacks of the above-mentioned methods, we have proposed coalescence-induced TDD reduction^{19,20} based on the following two key observations reported so far in SEG Ge growth^{7,15,21–23}: 1) TDs are bent to be normal to the growth surfaces (observed by the cross-sectional transmission electron microscope (TEM)), and 2) coalescence of SEG Ge layers results in the formation of semicylindrical voids over the SiO_2 masks.

We have assumed that the TDs are bent owing to the image force from the growth surface. In the case of Ge on Si, the image force generates 1.38 GPa and 1.86 GPa shear stresses for screw dislocations and edge dislocations at distances 1 nm away from the free surfaces, respectively¹⁹. The calculated shear stresses are significantly larger than the Peierls stress of 0.5 GPa reported

for 60° dislocations in Ge²⁴. The calculation predicts TDD reduction in Ge SEG layers on a quantitative basis and is in good agreement with the SEG Ge growth¹⁹. TEM observations of TDs are carried out to understand TD behaviors in the presented SEG Ge growth on Si²⁰. The image-force-induced TDD reduction is free from any thermal annealing or thick buffer layers, and thus is more suitable for photonic device application.

In this article, we describe specific methods for the theoretical calculation and experimental verification employed in the proposing TDD reduction method.

PROTOCOL:

1. Theoretical calculation procedure

1.1. Calculate trajectories of TDs. In the calculation, assume the SEG masks to be thin enough to ignore the ART effect on TDD reduction.

1.1.1. Determine growth surfaces and express them by equation(s). For instance, express the time evolution of a round-shaped cross-section of a SEG Ge layer with the time evolution parameter $n = i$, SEG Ge heights (h_i) and SEG Ge radii (r_i), as shown in the **Supplemental Video 1a** and Eq. (1):

$$x^2 + \{y - (r_i - h_i)\}^2 = r_i^2. \quad (1)$$

1.1.2. Determine normal directions for an arbitrary location on the growth surfaces. For the round-shaped cross-section SEG Ge, describe the normal line at (x_i, y_i) as $y = \frac{y_i - (h_i - r_i)}{x_i}x + h_i - r_i$, shown in **Supplemental Video 1b** as a red line. Then, obtain the edge of the TD (x_{i+1}, y_{i+1}) from the point (x_i, y_i) by solving the following simultaneous equations:

$$\begin{cases} x^2 + \{y - (r_{i+1} - h_{i+1})\}^2 = r_{i+1}^2 & (2a) \\ y = \frac{y_i - (h_i - r_i)}{x_i}x + h_i - r_i & (2b) \end{cases}$$

1.1.3. Calculate a trajectory of one TD depending on the location of TD generation $(x_0, 0)$, as shown in **Supplemental Video 1c**. In other words, a trajectory for an arbitrary TD can be calculated by the method described above.

1.1.4. Calculate TDD assuming that TDs penetrate to the bottom surface and contribute to the reduction of TDD (i.e., TDs below the point where SEG Ge layers coalesce are trapped by semicylindrical voids and never appear on the top surface).

2. Experimental verification procedure

2.1. SEG mask preparation

2.1.1. Prior to the fabrication of SEG masks, define Ge growth areas by preparing a design file. In the present work, prepare line-and-space patterns aligned to the [110] direction and square-shaped Si window areas of 4 mm in width using commercial software (e.g., AutoCAD).

2.1.2. Determine the design of SEG masks (in particular W_{window} and W_{mask}) using the software. W_{window} is the window width (Si seed width) and W_{mask} is the SiO_2 mask width, such that SEG Ge layers can coalesce with their adjacent ones. Determine W_{window} and W_{mask} by drawing rectangles by clicking **open file** → **structure** → **rectangle or polyline**.

NOTE: The width of the rectangles becomes W_{window} , and the interval of the rectangles becomes W_{mask} . In the present work, the minimum values of W_{window} and W_{mask} are 0.5 μm and 0.3 μm , respectively, which are restricted by the resolution in the employed EB lithography system.

2.1.3. As references, draw square-shaped Si window areas of 4 mm in width D , regarded as the blanket areas. Click **open file** → **structure** → **rectangle or polyline** to draw the square-shaped Si window. Use the schematics shown in **Figure 1** to prepare the line-and-space patterns and the 4 mm square blanket area.

2.1.4. Prepare B-doped p-Si (001) substrates with the resistivity of 1–100 $\Omega\cdot\text{cm}$. In the present work, use 4-inch Si substrates. Clean the substrate surfaces with Piranha solution (a mixture of 20 mL of 30% H_2O_2 and 80 mL of 96% H_2SO_4) as necessary.

2.1.5. Open the lid on a tube furnace and load the Si substrates into the furnace using a glass rod. In the present work, oxidize 10 Si substrates at one time.

2.1.6. Start to blow dry N_2 gas into the furnace by opening the gas valve. Then, set the gas flow rate to 0.5 L/m by controlling the valve.

2.1.7. Set the annealing temperature by changing the program. In the present work, use “pattern step (mode 2)” and set the process temperature to 900 $^\circ\text{C}$. Then, run the program by pushing **function** → **run**.

2.1.8. As the temperature reaches 900 $^\circ\text{C}$, close the dry N_2 valve, open the dry O_2 valve (O_2 flow = 1 L/m), and keep for 2 h.

NOTE: Perform steps 2.1.9–2.1.16 in a yellow room.

2.1.9. Coat the oxidized Si substrates with a surfactant (OAP) using a spin coater and then bake at 110 $^\circ\text{C}$ for 90 s on a hotplate.

2.1.10. After the surfactant coating, coat the Si substrates with a photoresist (e.g., ZEP520A) using a spin coater and then bake at 180 $^\circ\text{C}$ for 5 min on a hotplate.

2.1.11. Load the Si substrates with the surfactant and photoresist into an electron beam (EB) writer.

2.1.12. Read the design file (prepared in step 2.1.2) in the EB writer and make an operation file (WEC file). Set dose quantity as $120 \mu\text{C}/\text{cm}^2$ in the WEC file. As the substrate loading finishes, perform EB exposure by clicking the **single exposure** button.

2.1.13. Unload the substrate from the EB writer by clicking **wafer carry** → **unload** as the exposure finishes.

2.1.14. Prepare a photoresist developer (ZED) and a rinse for the developer (ZMD) in a draft chamber. Dip the exposed Si substrates into the developer for 60 s at room temperature.

2.1.15. Remove the Si substrates from the developer, and then dry the substrate with N_2 gas.

2.1.16. Put the developed Si substrates on a hotplate to bake at 110°C for 90 s.

2.1.17. Dip the Si substrates into a buffered hydrofluoric acid (BHF-63SE) for 1 min in order to remove part of the SiO_2 layers exposed to the air as the result of EB exposure and development.

2.1.18. Remove the photoresist from the Si substrates by dipping into an organic photoresist remover (e.g., Hakuri-104) for 15 min.

2.1.19. Dip the Si substrates into 0.5% diluted hydrofluoric acid for 4 min to remove the thin native oxide in the window regions but to retain the SiO_2 masks. Then load onto an ultrahigh-vacuum chemical vapor deposition (UHV-CVD) chamber to grow Ge. **Figure 2** shows the UHV-CVD system used in the present work.

2.2. Epitaxial Ge growth

2.2.1. Load the Si substrate with SEG masks (fabricated as in step 2.1) into a load lock chamber.

2.2.2. Set the buffer/main growth temperature in the **Recipe** tab shown on the operation computer. Determine the durations for the main growth of Ge so that SEG Ge layers coalesce with adjacent ones. To decide the durations for the main growth, consider the growth rate of Ge on the {113} planes, which determines the growth in the in-plane/lateral direction²⁶. In the present work, set the durations for the main growth as 270 min and 150 min for 650°C and 700°C , respectively.

2.2.3. Click **start** in main window, and then the Si substrate is automatically transferred into the growth chamber.

NOTE: Protocol on epitaxial Ge growth (steps 2.2.4–2.2.7) is automatically processed.

2.2.4. Grow Ge buffer on the loaded Si substrate at low-temperature ($\approx 380^\circ\text{C}$). Use GeH_4 diluted at 9% in Ar as the source gas and keep the partial pressure of GeH_4 for 0.5 Pa during the buffer growth.

2.2.5. Grow Ge main layer at an elevated temperature. Keep the partial pressure of GeH_4 for 0.8 Pa during the main growth. In the present work, use two different temperatures of 650 and 700 $^\circ\text{C}$ for the main growth temperature in order to compare SEG Ge with a round-shaped cross-section and with a {113}-facetted cross-section²⁵.

NOTE: The growth rate of Ge on the (001) plane was 11.7 nm/min independent of the temperature.

2.2.6. In order to visualize the evolution of SEG Ge and their coalescence, perform Ge growth with periodic insertion of 10-nm-thick $\text{Si}_{0.3}\text{Ge}_{0.7}$ demarcation layers on another Si substrate. $\text{Si}_{0.3}\text{Ge}_{0.7}$ layers were formed using Si_2H_6 and GeH_4 gases. During the $\text{Si}_{0.3}\text{Ge}_{0.7}$ -layer growth, set the partial pressure of Si_2H_6 gas at 0.02 Pa and the partial pressure of GeH_4 gas at 0.8 Pa.

2.2.7. As the Si substrate is automatically transferred from the growth chamber to the load lock chamber, vent the load lock chamber and unload the Si substrate manually.

2.3. Etch pit density (EPD) measurements

2.3.1. Dissolve 32 mg of I_2 in 67 mL of CH_3COOH using an ultrasonic cleaning machine.

2.3.2. Mix the I_2 -dissolved CH_3COOH , 20 mL of HNO_3 , and 10 mL of HF.

2.3.3. Dip the Ge-grown Si substrates into the $\text{CH}_3\text{COOH}/\text{HNO}_3/\text{HF}/\text{I}_2$ solution for 5–7 s in order to form etched pits.

2.3.4. Observe the etched Ge surfaces with an optical microscope (typically 100x) to ensure that etched pits are successfully formed.

2.3.5. Employ an atomic force microscope (AFM) to count the etched pits. Put the etched Ge sample on an AFM stage, and then approach the probe by clicking **auto approach**.

2.3.6. Decide the observation area using an optical microscope integrated with an AFM, and scan five different $10\ \mu\text{m} \times 10\ \mu\text{m}$ areas. The amplitude damping factor is automatically determined.

2.4. TEM observations

2.4.1. Pick up TEM specimens from the coalesced/blanket Ge layers by using a focused Ge ion beam (FIB micro sampling method)²⁷.

2.4.2. Polish the TEM specimens in an ion milling system using Ar ions. In the present work, thin

down TEM specimens for cross-sectional observations to be 150–500 nm in the [110] direction, and for plan-view observations to be 200 nm in the [001] direction.

2.4.3. For plan-view TEM specimens, protect the top surfaces of the Ge layers with amorphous layers, and then thin down from the bottom (substrate) side of the Ge layers.

2.4.4. Perform TEM observations under an acceleration voltage of 200 kV. Perform cross-sectional bright-field scanning TEM (STEM) observations in order to observe thick (500 nm) TEM specimens.

2.4.5. For a coalesced Ge with $\text{Si}_{0.3}\text{Ge}_{0.7}$ demarcation layers, perform cross-sectional high-angle annular dark field (HAADF) STEM observations under an acceleration voltage of 200 kV.

REPRESENTATIVE RESULTS:

Theoretical Calculation

Figure 3 shows calculated trajectories of TDs in 6 types of coalesced Ge layers: here, we define the aperture ratio (APR) to be $W_{\text{window}}/(W_{\text{window}} + W_{\text{mask}})$. **Figure 3a** shows a round-shaped SEG origin coalesced Ge of APR = 0.8. Here, 2/6 TDs are trapped. **Figure 3b** shows a {113}-facetted SEG origin coalesced Ge of APR = 0.8. Here, 0/6 TDs are trapped. **Figure 3c** shows a round-shaped SEG origin coalesced Ge of APR = 0.1. Here, 5/6 TDs are trapped. **Figure 3d** shows a {113}-facetted SEG origin coalesced Ge of APR = 0.1. Here, 6/6 TDs are trapped. **Figure 3e** shows a round-shaped SEG origin coalesced Ge of APR = 0.1, in case that Ge grows on SiO_2 masks. Here, 0/6 TDs are trapped. **Figure 3f** shows a {113}-facetted SEG origin coalesced Ge of APR = 0.1, in case that Ge grows on SiO_2 masks. Here, 0/6 TDs are trapped.

The trajectories of 6 TDs generated at $(x_0, 0)$, where $x_0 = 0.04, 0.1, 0.2, 0.4, 0.6$, and 0.8 times $W_{\text{window}}/2$, are shown as red lines in each figure. TDs located above the coalescence points of these two SEG Ge layers propagate upward to the top surface, while TDs below the points propagate downward to remain at the void surface over the SiO_2 mask.

In **Figure 3a–3d**, it is assumed that SEG Ge does not grow on SiO_2 . Thus, the sidewalls of the {113}-facetted SEG Ge are assumed to be round-shaped in order to not touch the SiO_2 masked area. It is clearly shown that round-shaped SEG and then coalesced Ge are more effective to reduce TDD at an APR of 0.8, than the {113}-facetted case, while {113}-facetted and then coalesced Ge are more effective than a round-shaped one at an APR of 0.1. This “crossing” is ascribed to the presence of {113} facets near the SEG top: {113} facets are more deviated from the [001] direction than round-shaped surfaces.

Figure 3e and Figure 3f show coalesced Ge at an aperture ratio of 0.1, assuming that Ge is not nucleated on SiO_2 but shows wetting with the SiO_2 mask, widely reported in previously reported Ge coalescence^{13,15,22,28–31}. As shown in **Figure 3e and Figure 3f**, there is no semi cylindrical void between two SEG and thus no TD is trapped at the surface.

Figure 4 shows calculated TDDs in coalesced Ge. In **Figure 4**, the red line shows calculated TDDs

in coalesced Ge originating from the round-shaped SEG Ge, and the blue line shows calculated TDDs in coalesced Ge originating from the {113}-facetted SEG Ge. Since TDs in Ge on Si originate from the lattice mismatch between Ge and Si, it is assumed that TD generation occurs only at interfaces between Ge and Si. In other words, TDD should be reduced with APR.

When APR is larger than 0.11, the round-shaped SEG Ge is more effective than the {113}-facetted one (**Figure 3a and Figure 3b**). When APR is smaller than 0.11, on the other hand, the {113}-facetted SEG Ge becomes more effective than the round-shaped one (**Figure 3c and Figure 3d**). As in **Figure 3**, such crossing is ascribed to the presence of {113} facets near the SEG top ($x_0 \approx 0$). Note that **Figure 3e and Figure 3f** correspond to the black line in **Figure 4**, showing the reduction of TDD from the reduction of APR, but not to the coalescence (i.e., SEG Ge wetting with SiO₂ has a negative effect against the TDD reduction).

Experimental Verification

Figure 5 show typical cross-sectional scanning electron microscopy (SEM) images (**Figure 5b–5d, 5f**) and the distribution maps (**Figure 5a, 5e**) showing whether coalescence occurs or not. **Figure 5b–5d, 5f** show cross-sectional SEM images of non-coalesced SEG Ge layers (**Figure 5b**, grown at 700 °C; **Figure 5f**, grown at 650 °C), coalesced SEG Ge layers with a non-flat top surface (**Figure 5c**, grown at 700 °C), and coalesced SEG Ge layers with a flat top surface (**Figure 5d**; grown at 700 °C). SEM images shown in **Figure 5b** and **Figure 5d** are polished by a focused ion beam after deposition of Pt protection layers. The coalescence occurs when the W_{window} and W_{mask} are smaller than 1 μm for the present growth conditions. The SEG masks with W_{mask} of 1 μm or larger prevent the coalescence of Ge due to the small amount of Ge growth in the lateral direction²⁶. The SEG masks with a W_{window} of 2 μm or greater also prevent the coalescence of Ge, although the coalescence took place when the W_{window} is smaller than 1 μm. This is because the lateral growth rate of Ge over SiO₂ depends on the W_{window} ³⁰. The mask and window pattern dependence are summarized in **Figure 7a** (700 °C) and **Figure 7e** (650 °C).

Comparing the non-coalesced SEG Ge layers (**Figure 4b and Figure 4f**), it is clearly shown that the SEG Ge layer grown at 700 °C has a round-shaped cross-section while the SEG Ge layer grown at 650 °C has a {113}-facetted cross-section. As in **Figure 5b**, the growth at 700 °C shows a round-shaped SEG Ge without Ge growth on SiO₂ (i.e., no wetting with the SiO₂ mask). Therefore, the growth proceeds like **Figure 3a and Figure 3c**. On the other hand, as in **Figure 5f**, an {113}-facetted SEG Ge appears at 650 °C. It is strongly suggestive that the Ge would show wetting with the SiO₂ mask. In contrast, the edge is round-shaped (i.e., not wetting). Therefore, the growth at 650 °C is in between **Figure 3b** (no wetting) and **Figure 3f** (perfect wetting). This indicates that the TDD reduction should be in between **Figure 3b** and **Figure 3f**. Considering the theoretical results shown in **Figure 6**, these differences in the SEG Ge cross-sections should strongly influence TDDs in the coalesced Ge layers.

The difference in wetting growth on SiO₂ can be understood as follows. The contact angle between Ge and SiO₂ (θ) is determined by Young's equation:

$$\gamma_{\text{SiO}_2} = \gamma_{\text{Ge}} \cos \theta + \gamma_{\text{int}} \quad (4)$$

Here, γ_{SiO_2} , γ_{Ge} , and γ_{int} are SiO_2 surface free energy, Ge surface free energy, and Ge/ SiO_2 interfacial free energy, respectively. The angle of the SEG Ge sidewall becomes larger as Ge growth proceeds. When the angle of the SEG Ge sidewall reaches the contact angle θ , the SEG Ge needs to grow in the vertical ([001]) or lateral ($[1\bar{1}0]$) direction. In the case for 650 °C growth, the vertical growth is severely limited by the {113} facets, and thus SEG Ge prefers to grow in lateral direction (i.e., wetting growth). Even though the wetting could generate dislocations at the Ge and SiO_2 interface, it is finally to be terminated at the semicylindrical void surface. In the case for 700 °C growth, Ge can grow in a vertical direction, and the contact angle is larger than that for 650 °C because of a larger γ_{int} . This would be the reason why 650 °C-grown Ge shows wetting over SiO_2 while 700 °C grown-Ge does not.

For Ge after coalescence, the cross-sectional structure is not influenced by the growth temperature: coalesced Ge layers grown at 650 °C and the ones grown at 700 °C could not be differentiated by cross-sectional SEM observations.

Note that for the fabricated patterns, W_{window} values were larger and W_{mask} values were smaller than the designed ones because an isotropic wet etching process was employed to fabricate the mask. The actual values of W_{window} and W_{mask} were obtained by cross-sectional SEM observations after Ge growth.

In addition to that, the thickness of the mask SiO_2 layers was 30 nm according to the cross-sectional SEM observations and spectroscopic ellipsometry measurements. Such thin SiO_2 layers were employed to examine the TDD reduction explained in **Figure 3** and **Figure 4**, removing the effect of epitaxial necking on the ART. In the present work, the aspect ratios are lower than 0.05, which is small enough to ignore the effect of epitaxial necking on the ART.

Figure 6a shows a cross sectional HAADF STEM for a SEG with $Si_{0.3}Ge_{0.7}$ demarcation layers, and a schematic illustration of **Figure 6a** is shown in **Figure 6b** ($W_{window} = 0.66 \mu m$, $W_{mask} = 0.84 \mu m$). The $Si_{0.3}Ge_{0.7}$ demarcation layers clearly show the surface shapes during the growth at 700 °C. The STEM image shows the Ge surfaces of each growth step from round-shaped SEG to a flat epitaxial layer formed after the coalescence. The growth rate just after coalescence is strongly enhanced at the coalesced areas. This rapid growth is probably induced by the Ge epilayer, minimizing its surface area to get energetically stabilized.

In contrast to the pure Ge SEG, the presented Ge SEG with the $Si_{0.3}Ge_{0.7}$ demarcation layers show wetting with the SiO_2 masks (**Figure 8a**). The difference in wetting is perhaps due to the insertion of $Si_{0.3}Ge_{0.7}$ demarcation layers, whose nucleation is enhanced on SiO_2 layers unlikely that of Ge.

Flat-top coalesced Ge (blue-circled areas in **Figure 5a** and **Figure 5e**) are used for EPD measurements. The Ge layers were etched on average by 200 nm. Typical AFM images after etching are shown in **Figure 7a** and **Figure 7b**, taken for 1.15- μm -thick coalesced Ge grown at 700 °C ($W_{window} = 0.66 \mu m$ and $W_{mask} = 0.44 \mu m$) and 2.67- μm -thick coalesced Ge grown at 650 °C ($W_{window} = 0.66 \mu m$ and $W_{mask} = 0.34 \mu m$). As a reference, the image of the 1.89- μm -thick blanket

Ge grown at 700 °C is shown in **Figure 7c**. The dark dots in the AFM images are etched pits indicating the presence of TDs. The EPD values from **Figure 7a-7c** were obtained to be $7.0 \times 10^7/\text{cm}^2$, $7.9 \times 10^7/\text{cm}^2$, and $8.7 \times 10^7/\text{cm}^2$, respectively. Our previous reports showed that the obtained EPDs in this etching condition are equal to TDDs determined by plan-view transmission electron microscopy (TEM)^{4,32-34}. The measured EPD of blanket Ge layer ($7.9 \pm 0.8 \times 10^7/\text{cm}^2$) agrees well with TDD obtained from plan-view TEM observation with a relatively large area of $6 \times 8 \mu\text{m}^2$ ($8.7 \pm 0.2 \times 10^7/\text{cm}^2$), indicating that the EPD is equal to TDD.

In order to compare the experimentally obtained TDDs with calculations, take into account the effect of thickness on TDD. There is a trend that TDD decreases as the Ge thickness increases because of increased chances for the pair annihilation of TDs. Therefore, the reduction of TDD observed for the coalesced Ge, thinner than blanket Ge, should be ascribed to the mechanism described in **Figure 3 and Figure 4** (i.e., we need to calculate the normalized TDD to compare the experimentally obtained TDDs with the calculated ones in **Figure 4**). Before the normalization, a correction of TDD for blanket Ge (ρ_{blanket}) was performed, considering the thickness and the growth temperature on TDD. Similar to the previous reports^{35,36}, $\rho_{\text{blanket}} [/\text{cm}^2]$ is approximately expressed as $2.52 \times 10^{13} \times [d (\text{nm})]^{-1.57}$ for the Ge layers grown in the temperature range of 530–650 °C using a UHV-CVD. Here, d is the thickness of the blanket Ge layer. $\rho_{\text{blanket}} [/\text{cm}^2]$ is reduced for the Ge layers grown at 700 °C, and approximately expressed as $2.67 \times 10^{12} \times [d (\text{nm})]^{-1.37}$.

Figure 7d shows the normalized TDD as a function of APR, $W_{\text{window}}/(W_{\text{window}} + W_{\text{mask}})$. TDDs in coalesced Ge grown at 650 °C are shown as blue triangles and those grown at 700 °C as red diamonds. Since SEG Ge at 650 °C shows some wetting with the SiO_2 mask, the growth data should fall in between the black and blue lines. SEG Ge at 700 °C should be on the red line. The experimental results are in good agreement with the calculation based on the cross-sectional shape and wetting conditions.

As described above, it is concluded that the behavior of TDs is well explained by the model based on the image force of growth surfaces on TDs. In order to understand the interaction of TD with the surface, we have observed TDs with a bright-field cross sectional STEM. A defect is observed being bent and terminated on a surface of a semicylindrical void in **Figure 8a**. This behavior of the TD is quite similar to calculated trajectories of TDs shown in **Figure 3**. However, the observed trajectory of TD does not exactly reproduce the one we predicted in **Figure 3**. The difference would be explained as the result of a TD transformation in order to minimize its energy during or after the growth (e.g., temperature decrease from growth temperature to room temperature). **Figure 8b** shows a simulation of strain in the coalesced Ge epilayer on Si. Tensile strain is induced in the Ge layer on Si because of the mismatch of thermal expansion coefficient between Ge and Si. The simulation indicates that strain accumulation occurs at the top of the semicylindrical voids and strain relaxation at the sub-surface layer of the semicylindrical voids, which would motivate TDs to transform.

On the other hand, **Figure 8c** shows defect generation at the top of a void, although the generation point would be removed during the preparation of the TEM specimen. The defect in **Figure 8c** is close to a straight line, but the angle between the defect and (001) plane ($\approx 78.3^\circ$)

does not agree with that for the {111} plane (54.7°).

The electron diffraction pattern shown in **Figure 8d** was obtained near the defect in **Figure 8c**. The absence of streak light indicates that there should not be a 2D structure (i.e., the defect is a dislocation). In previous reports^{28-31,37}, 2D defects were formed showing clear a streak light in electron diffraction patterns, which is against the one observed in the present work. The observation results (the absence of 2D defects) supports the prediction that the voids and their free surfaces contribute to release strain in Ge on Si, or otherwise cause the crystal misorientations between adjacent SEG Ge layers. This is consistent with a previous report briefly suggesting that the formation of 2D defects is prevented in coalesced SEG Ge layers with voids on the SiO₂ masks³⁸.

There are two candidates for the TD generation shown in **Figure 10c**: the strain distribution and the misorientation between SEG Ge layers. In epitaxial Ge on Si, the tensile strain is induced in Ge due to the mismatch of thermal expansion coefficient between Ge and Si³⁹. The simulation result shown in **Figure 8b** indicates accumulation of tensile-strain (~0.5%) at the top of the void as mentioned above. Such strain accumulation at the void top could result in TD generation shown in **Figure 8c**. Another candidate, the misorientation between SEG Ge layers, has been assumed to generate 2D defects as observed in previous reports showing coalescence of SEG Ge layers^{28-31,37}. In the present work, however, the generation of 2D defects would be suppressed owing to the presence of voids as briefly mentioned in a previous report³⁸, but result in the TD generation owing to imperfect suppression. More detailed discussion for the misorientation-induced dislocation will be described in a later part with schematic illustrations (**Figure 12**).

Figure 9a and **Figure 9b** show bright-field plan-view TEM images of a coalesced Ge layer ($W_{\text{window}} = 0.82 \mu\text{m}$, $W_{\text{mask}} = 0.68 \mu\text{m}$) and a blanket Ge layer, respectively, grown on the same substrate. For the plan-view TEM observations, TEM specimens were formed using the top 200 nm regions of the Ge layers as described in step 2.4.3 and are indicated by red dashed squares in the schematic cross-sections at the top of **Figure 9**. SiO₂ mask stripes are aligned to the [110] direction for the coalesced Ge in **Figure 9a**. The plan-view TEM image shown in **Figure 9a** was taken for a $6 \mu\text{m} \times 8 \mu\text{m}$ area. Although there are five pairs of SiO₂ masks and Si window areas in this TEM image, the areas above the SiO₂ masks and Si windows are not distinguishable in the TEM image. This is because the observed area (top 200 nm) is far above where semicylindrical voids are located (bottom 150 nm).

It is found that TDDs obtained from **Figure 9a** and **Figure 9b** are $4.8 \times 10^7/\text{cm}^2$ and $8.8 \times 10^7/\text{cm}^2$, respectively. As shown in **Figure 7d**, EPD measurements reveal that TDD in the coalesced Ge layer ($W_{\text{window}} = 0.82 \mu\text{m}$ and $W_{\text{mask}} = 0.68 \mu\text{m}$) is $4 \times 10^7 \text{ cm}^{-2}$. Thus, the TDD in **Figure 9a** shows a good agreement with the EPD shown in **Figure 7**. It is also notable that neither EPD measurements nor TEM observations show TDD re-increase, which is frequently shown when SEG Ge layers coalesce (i.e., the TDD re-increase owing to generation of TDs (**Figure 8b**) is suppressed to such an extent that the TDD re-increase is ignorable in the present TDD range (on the order of $10^7/\text{cm}^2$)).

It should be remarked that a TD-free area as large as $4 \mu\text{m} \times 4 \mu\text{m}$ is realized in the coalesced Ge,

as in **Figure 9a**. Although the blanket Ge in **Figure 9b** shows TDs with a relatively uniform distribution, the coalesced Ge has high and low TDD areas. Such differences in TD distribution suggest that further TDD reduction would be achievable in the coalesced Ge. 1 TD in a $4\ \mu\text{m} \times 4\ \mu\text{m}$ area, which is observed in **Figure 9a**, corresponds to TDD of $6.25 \times 10^6/\text{cm}^2$.

Comparing coalesced Ge (**Figure 9a**) and blanket Ge (**Figure 9b**), it is clear that the lengths of the defect lines in coalesced Ge are longer than those in blanket Ge. In coalesced Ge, there are typically $1\text{-}\mu\text{m}$ -long defect lines, and they are aligned to the $[110]$ direction. Note that the $[110]$ direction is the length direction of the SiO_2 stripes. There are two possible explanations for such long defect lines: (i) 2D defects are observed and (ii) dislocations are inclined in the $[110]$ direction. However, 2D defects are immediately denied because of the widths of the observed long defects (i.e., 2D defects on $\{111\}$ planes should show wider defect lines). Geometrically, 2D defects on the $\{111\}$ planes should show 140-nm -wide defect lines, taking into account the thickness of the TEM specimen (200 nm) and the angle of the $\{111\}$ with (001) planes (54.7°). The plan-view TEM image shows that the defect lines are $10\text{--}20\text{ nm}$ in width, which is much narrower than 140 nm . Thus, the defects shown as long lines should be ascribed to (ii) dislocations inclined in the $[110]$ direction. A simple geometrical calculation gives the angle between the inclined dislocations and (001) planes: $\tan^{-1}(200\text{ nm}/1\ \mu\text{m}) = 11.3^\circ$. Note that, as shown in **Figure 8b**, TDs in blanket Ge tend to be directed almost vertical to the substrate if no post-growth annealing is performed, showing small black dots in plan-view TEM images.

For more detailed analysis of the inclined TDs, a small area with high-TDD is arbitrarily observed as in **Figure 10**. The TEM specimen was prepared from the top 200 nm of the coalesced Ge layer, the same as the plan-view TEM observations above.

Figure 10a and **Figure 10b** show dark-field ($\mathbf{g} = [220]$ for **Figure 10a** and $[2\bar{2}0]$ for **Figure 10b**) plan-view TEM images taken at the same area. In **Figure 10a**, four inclined dislocations were observed in a $4\ \mu\text{m} \times 4\ \mu\text{m}$ area. **Figure 10b** reveals that one inclined dislocation (the red-circled one) disappears when diffraction vector $\mathbf{g} = [2\bar{2}0]$, which indicates that the Burgers vector is determined to be $[110]$ or $[1\bar{1}0]$ for the red-circled dislocation. Since the defect line is in the $[110]$ direction, the dislocation is found to be a screw dislocation. The other three inclined dislocations (green-circled ones) are ascribed to the mixed dislocations because they did not disappear whatever diffraction vector \mathbf{g} was chosen.

There are two possible explanations for the inclination of TDs in coalesced Ge layers: (i) Ge growth in $[110]$ direction, and (ii) defect generation when SEG Ge layers coalesce.

Ge growth in $[110]$ direction

Figure 11 shows a plan-view SEM image and the growth process to form a flat epitaxial layer from a non-planar SEG surface as a schematic movie. Reflecting the edge undulation of the SiO_2 stripe patterns formed by the EB lithography and wet chemical etching, the coalescence preferentially starts at some points, and then proceeds in the $[110]$ and $[\bar{1}\bar{1}0]$ directions above the SiO_2 masks. **Figure 11b** and **Figure 11c** schematically show the bird's eye view and the $(1\bar{1}0)$ cross-sectional view when SEG Ge layers are partly coalesced. A TD generated at a growth window appears above

the void as shown in **Figure 3**, and then the TDs start to propagate in the $[110]$ or $[\bar{1}\bar{1}0]$ direction due to the image force. This leads to TDs inclined in the $[110]$ direction (as in **Figure 9a**). The red solid line in **Figure 11c** shows a TD bent in the $[110]$ direction according to the model above, which explains the presence of the inclined TDs observed in **Figure 9a** and **Figure 10** on a qualitative basis.

The mechanism can explain both edge and screw TDs, taking into account the Burgers vectors of TDs generated at Ge/Si interfaces⁴⁰. As Ge is grown on a Si substrate, edge misfit dislocations (MDs) are formed to release strain, and MDs are aligned in the $[110]$ or $[\bar{1}\bar{1}0]$ direction. The MDs form threading segments (i.e., TDs), and the Burgers vectors for the TDs originated from MDs aligned in the $[110]$ direction (MD_{110}) are $a/2[\bar{1}\bar{1}0]$ or $a/2[\bar{1}10]$ (a : the lattice constant). On the other hand, the Burgers vectors are $a/2[110]$ or $a/2[\bar{1}\bar{1}0]$ for the TDs originated from MDs aligned in the $[\bar{1}\bar{1}0]$ direction ($MD_{\bar{1}\bar{1}0}$). In the case that the TDs from MD_{110} are inclined to the $[110]$ direction, plan-view TEM observations show the TDs as edge dislocations. Similarly, when the TDs from $MD_{\bar{1}\bar{1}0}$ are inclined to the $[110]$ direction, they are observed as screw dislocations.

Defect generation when SEG Ge layers coalesce

Figure 12 shows schematics explaining generation of defects when SEG Ge layers coalesce with small rotation (i.e., misorientation). As schematically illustrated in **Figure 12**, the misorientation should generate edge/screw/mixed dislocations at the coalescence interface. In **Figure 12**, misorientation between two SEG Ge layers in the $[110]$ direction is decomposed into three types of rotations. **Figure 12a-12c** shows the rotation around the $[110]$ axis, the $[001]$ axis, and the $[\bar{1}\bar{1}0]$ axis, respectively.

The coalescence in **Figure 12** is assumed to occur between a strictly epitaxial Ge layer (Ge (001)) and an adjacent SEG Ge layer with a misorientation (m-Ge). The rotation around the $[110]$ axis (**Figure 12a**) results in the generation of edge dislocations parallel to the $[110]$ direction at the boundary indicated as a dashed line. Similarly, as in **Figure 12b**, the edge dislocations parallel to the $[001]$ direction are generated as a result of the rotation around the $[001]$ axis. On the other hand, the rotation around the $[\bar{1}\bar{1}0]$ axis, shown in **Figure 12c**, generates a screw dislocation network, which is composed by dislocations of $\mathbf{b} = [110]$ and $\mathbf{b} = [001]$, being similar to the case for direct bonding of Si (001) surfaces showing screw dislocation network⁴¹. The screw TD observed in **Figure 10** could be ascribed to the coalescence with misorientation of a rotation around $[\bar{1}\bar{1}0]$ axis. The combination of rotations around $[110]$ axis (**Figure 12a**) and around $[\bar{1}\bar{1}0]$ axis (**Figure 12c**) can explain the mixed TDs shown in **Figure 12**. The mixed dislocation shown in **Figure 9b** is also explained by the combination of the rotation around the $[001]$ axis (**Figure 12b**) and the rotation on the $[\bar{1}\bar{1}0]$ axis (**Figure 12c**).

Assuming that the dislocations originated from the misorientation are generated at a density of $1 \times 10^7/\text{cm}^2$, the average angle of the rotation around $[\bar{1}\bar{1}0]$ axis is estimated to be 0.034° ⁴². Compared to the estimation, we have already reported that there are fluctuations of orientation in a line-shaped SEG Ge layer for 100 arcsec ($= 0.028^\circ$), employing micro-beam X-ray diffraction observations⁴³. The reported fluctuations of orientation and estimated rotation angle show good agreement, which supports the TD generation mechanism based on misorientations.

FIGURE AND TABLE LEGENDS:

Figure 1: Schematic illustrations of line-and-space shaped and 4 mm square SEG masks on a Si(001) substrate.

Figure 2: Pictures for parts of an UHV-CVD machine; gas cabinet, process chamber, load lock chamber, and operation computer.

Figure 3: Calculated trajectories of 4 TDs in (a) round-shaped SEG origin, aperture ratio = 0.8, (b) round-shaped SEG origin, aperture ratio = 0.1, (c) {113}-facetted SEG origin, aperture ratio = 0.8, and (d) {113}-facetted SEG origin, aperture ratio = 0.1.

Figure 4: Calculated TDDs in coalesced Ge originated from {113}-facetted SEG Ge (blue line) and round-shaped SEG Ge (red line).

Figure 5: Distribution maps and SEM images of coalesced/non-coalesced Ge layers.

Figure 6: (a) A cross-sectional HAADF STEM image of coalesced Ge ($W_{\text{window}} = 0.66 \mu\text{m}$, $W_{\text{mask}} = 0.84 \mu\text{m}$) grown at 700 °C with 10-nm-thick $\text{Si}_{0.3}\text{Ge}_{0.7}$ demarcation layers, and (b) a schematic illustration corresponding to the conditions shown in (a).

Figure 7: Typical AFM images in order to measure EPDs for (a) 1.15- μm -thick coalesced Ge grown at 700 °C ($W_{\text{window}} = 0.66 \mu\text{m}$ and $W_{\text{mask}} = 0.44 \mu\text{m}$), (b) 2.67- μm -thick coalesced Ge grown at 650 °C ($W_{\text{window}} = 0.86 \mu\text{m}$ and $W_{\text{mask}} = 0.34 \mu\text{m}$), and (c) 1.89- μm -thick blanket Ge grown at 700 °C, and summary of the EPD measurement results in (d).

Figure 8: (110) cross-sectional (a) STEM and (b) TEM images of coalesced Ge layers ($W_{\text{window}} = 0.66 \mu\text{m}$ and $W_{\text{mask}} = 0.44 \mu\text{m}$), (c) electron diffraction pattern obtained near the defect shown in (b), and (d) finite element method simulation result of a strain distribution in the coalesced Ge. Figures 9(a), (c), and (d) have been modified from ²⁰.

Figure 9: Bright-field plan-view TEM images of (a) a coalesced Ge layer ($W_{\text{window}} = 0.82 \mu\text{m}$, $W_{\text{mask}} = 0.68 \mu\text{m}$) and (b) a blanket Ge layer.

Figure 10: Plan-view TEM images of a high-TDD small area with g vectors of (a) [220] and (b) $[\bar{2}\bar{2}0]$. This figure has been modified from ²⁰.

Figure 11: (a) A plan-view SEM image, (b) a bird's eye schematic image, and (c) a $(1\bar{1}0)$ cross-sectional schematic image of a partially coalesced SEG Ge. This figure has been modified from ²⁰.

Figure 12: Schematics of defect generation when SEG Ge layers coalesce with crystal rotation around (a) [110], (b) [001], and (c) $[1\bar{1}0]$ orientation. This figure has been modified from ²⁰.

Table 1: A summary of achieved TDD and drawbacks in view of photonic device application for conventional/presented TDD reduction methods.

Supplemental Figure 1: Four typical methods widely employed to reduce TDD in epitaxial Ge on Si: (a) thermal annealing, (b) SiGe graded buffer, (c) Aspect ratio trapping (ART), and (d) Si pillar seeds.

Supplemental Video 1: Schematic illustrations of a TD bent owing to image force in a round-shaped SEG Ge.

DISCUSSION:

In the present work, TDD of $4 \times 10^7/\text{cm}^2$ were experimentally shown. For further TDD reduction, there are mainly 2 critical steps within the protocol: SEG mask preparation and epitaxial Ge growth.

Our model shown in **Figure 4** indicates that TDD can be reduced lower than $10^7/\text{cm}^2$ in coalesced Ge when APR, $W_{\text{window}}/(W_{\text{window}} + W_{\text{mask}})$, is as small as 0.1. Toward further TDD reduction, SEG masks with smaller APR should be prepared. As mentioned in step 2.1.2, the minimum values of W_{window} and W_{mask} were 0.5 μm and 0.3 μm , respectively, limited by the resolution in the employed EB lithography system. One simple method to reduce APR is to modify lithography and etching processes (e.g., to use another photoresist, to use better lithography system, to use thinner SiO_2 layers with shallower BHF etching, etc.). Mature lithography and etching process will enable SEG masks narrower than 100 nm. In the present work, coalesced Ge with a flat top surface were obtained when $W_{\text{mask}} \leq 1 \mu\text{m}$. Thus, W_{window} of 100 nm and W_{mask} of 900 nm (APR = 0.1) will give us coalesced Ge with flat top surface in the present growth conditions.

In addition to that, the modification of SEG mask preparation should bring less edge undulation of SEG masks, resulting in suppression of misorientation between Ge SEG layers. The TD generation when SEG Ge layers coalesce (**Figure 11**) will be suppressed as the result of the modification of SEG mask preparation.

As revealed by calculation results (**Figure 3**), suppression of Ge growth on SiO_2 is required to reduce TDD. The suppression of Ge growth on SiO_2 is brought by modification of Ge growth step (i.e., elevation of growth temperature, rotation of SEG mask, introduction of H_2 gas, and reduction of the pressure of GeH_4 gas^{44,45}).

The TDD reduction method proposed/verified in the present work is superior to existing methods in terms of application for Ge photonic devices (i.e., TDD is reduced without any thermal annealing nor thick buffer layers). The maximum process temperature was 700 $^\circ\text{C}$, which is the growth temperature, and the height of the void was ≈ 150 nm. Compared with existing methods, the maximum temperature is lower than annealing temperature (typically 900 $^\circ\text{C}$)⁷, and height of the void is shallower than SiGe graded buffer layers (typically several μm)¹⁰, SiO_2 trenches for ART (typically 0.5–1 μm)¹³, and buffer layer for Ge growth on Si pillars (typically $\approx 5 \mu\text{m}$)¹⁸. The

comparison of conventional/presented methods are summarized in **Table 1**.

Considering the footprint of a typical Ge photonic device ($\approx 100 \mu\text{m}^2$), TDD lower than $10^6/\text{cm}^2$, and a number of TD $< 1/\text{device}$ will be the final goal. Since the theoretical limit of TDD for this method is 0, TDD lower than $10^6/\text{cm}^2$ is potentially achievable. Toward the goal, more optimized lithography and etching will be investigated.

ACKNOWLEDGMENTS:

This work was financially supported by Japan Society for the Promotion of Science (JSPS) KAKENHI (17J10044) from the Ministry of Education, Culture, Sports, Science and Technology (MEXT), Japan. The fabrication processes were supported by "Nanotechnology Platform" (project No. 12024046), MEXT, Japan. The authors would like to thank Mr. K. Yamashita and Ms. S. Hirata, the University of Tokyo, for their help on TEM observations.

DISCLOSURES:

The authors have nothing to disclose.

REFERENCES:

- [1] Giovane, L. M., Luan, H.-C., Agarwal, A. M., Kimerling, L. C. Correlation between leakage current density and threading dislocation density in SiGe p-i-n diodes grown on relaxed graded buffer layers. *Applied Physics Letters*. **78** (4), 541–543 (2001).
- [2] Wang J., Lee, S. Ge-photodetectors for Si-based optoelectronic integration. *Sensors*. **11**, 696–718 (2011).
- [3] Ishikawa Y., Saito, S. Ge-on-Si photonic devices for photonic-electronic integration on a Si platform. *IEICE Electronics Express*. **11** (24), 1–17 (2014).
- [4] Cai, Y., Materials science and design for germanium monolithic light source on silicon, Ph.D. dissertation, Dept. Mater. Sci. Eng., Massachusetts Inst. Technol., Cambridge, MA, USA (2009).
- [5] Wada K., Kimerling, L. C. Photonics and Electronics with Germanium. Hoboken, NJ, USA: Wiley, 294 (2015).
- [6] Higashitarumizu N., Ishikawa, Y. Enhanced direct-gap light emission from Si-capped n^+ -Ge epitaxial layers on Si after post-growth rapid cyclic annealing: Impact of non-radiative interface recombination toward Ge/Si double heterostructure lasers. *Optics Express*. **25** (18), 21286–21300 (2017).
- [7] Luan, H.-C. et al. High-quality Ge epilayers on Si with low threading-dislocation densities. *Applied Physics Letters*. **75** (19), 2909–2911 (1999).
- [8] Nayfeh, A., Chui, C. O., Saraswat, K. C. Effects of hydrogen annealing on heteroepitaxial-Ge layers on Si: Surface roughness and electrical quality. *Applied Physics Letters*. **85** (14), 2815–2817 (2004).
- [9] Choi, D., Ge, Y., Harris, J. S., Cagnon, J., Stemmer, S. Low surface roughness and threading dislocation density Ge growth on Si (001). *Journal of Crystal Growth*. **310** (18), 4273–4279 (2008).
- [10] Currie, M. T., Samavedam, S. B., Langdo, T. A., Leitz, C. W., Fitzgerald, E. A. Controlling threading dislocation densities in Ge on Si using graded SiGe layers and chemical-mechanical polishing. *Applied Physics Letters*. **72** (14), 1718–1720 (1998).
- [11] Liu, J. L., Tong, S., Luo, Y. H., Wan, J., Wang, K. L. High-quality Ge films on Si substrates using

- Sb surfactant-mediated graded SiGe buffers. *Applied Physics Letters*. **79** (21), 3431–3433 (2001).
- [12] Yoon, T.-S., Liu, J., Noori, A. M., Goorsky, M. S., Xie, Y.-H. Surface roughness and dislocation distribution in compositionally graded relaxed SiGe buffer layer with inserted-strained Si layers. *Applied Physics Letters*. **87** (1), 012014 (2005).
- [13] Langdo, T. A., Leitz, C. W., Currie, M. T., Fitzgerald, E. A. Lochtefeld, A., Antoniadis, D. A. High quality Ge on Si by epitaxial necking. *Applied Physics Letters*. **76** (25), 3700-3702 (2000).
- [14] Park, J.-S., Bai, J., Curtin, M., Adekore, B., Carroll, M., Lochtefeld, A. Defect reduction of selective Ge epitaxy in trenches on Si(001) substrates using aspect ratio trapping. *Applied Physics Letters*. **90** (5), 052113 (2007).
- [15] Fiorenza, J. G. et al. Aspect ratio trapping: A unique technology for integrating Ge and III-Vs with silicon CMOS. *ECS Transactions*. **33** (6), 963–976 (2010).
- [16] Salvalaglio, M. et al. Engineered Coalescence by Annealing 3D Ge Microstructures into High-Quality Suspended Layers on Si. *Applied Materials & Interfaces*. **7** (34), 19219–19225 (2015).
- [17] Bergamaschini, R. et al. Self-aligned Ge and SiGe three-dimensional epitaxy on dense Si pillar arrays. *Surface Science Reports*. **68** (3), 390-417 (2013).
- [18] Isa, F. et al. Highly Mismatched, Dislocation-Free SiGe/Si Heterostructures. *Advanced Materials*. **28** (5), 884–888 (2016).
- [19] Yako, M., Ishikawa, Y., Wada, K. Coalescence induced dislocation reduction in selectively grown lattice-mismatched heteroepitaxy: Theoretical prediction and experimental verification. *Journal of Applied Physics*. **123** (18), 185304 (2018).
- [20] Yako, M., Ishikawa, Y., Abe, E., Wada, K. Defects and Their Reduction in Ge Selective Epitaxy and Coalescence Layer on Si With Semicylindrical Voids on SiO₂ Masks. *IEEE Journal of Selected Topics in Quantum Electronics*. **24** (6), 8201007 (2018).
- [21] Park, J.-S., Bai, J., Curtin, M., Carroll, M., Lochtefeld, A. Facet formation and lateral overgrowth of selective Ge epitaxy on SiO₂-patterned Si(001) substrates. *Journal of Vacuum Science & Technology B*. **26** (1), 117–121 (2008).
- [22] Bai, J. et al. Study of the defect elimination mechanisms in aspect ratio trapping Ge growth. *Applied Physics Letters*. **90** (10), 101902 (2007).
- [23] Montalenti, F. et al. Dislocation-Free SiGe/Si Heterostructures, *Crystals*. **8** (6), 257 (2018).
- [24] Zhang, H. L. Calculation of shuffle 60° dislocation width and Peierls barrier and stress for semiconductors silicon and germanium. *European Physical Journal B*. **81** (2), 179–183 (2011).
- [25] Kim, M., Olubuyide, O. O., Yoon, J. U., Hoyt, J. L. Selective Epitaxial Growth of Ge-on-Si for Photodiode Applications. *ECS Transactions*. **16** (10), 837–847 (2008).
- [26] Yako, M., Kawai, N. J., Mizuno, Y., Wada, K. The kinetics of Ge lateral overgrowth on SiO₂, in *Proceedings of MRS Fall Meeting* (2015).
- [27] Kamino T., Yaguchi T., Hashimoto T., Ohnishi T., Umemura K. A FIB Micro-Sampling Technique and a Site Specific TEM Specimen Preparation Method. *Introduction to Focused Ion Beams*. Springer, Boston, MA (2005).
- [28] Park, J.-S. et al. Low-defect-density Ge epitaxy on Si(001) using aspect ratio trapping and epitaxial lateral overgrowth. *Electrochemical and Solid-State Letters*. **12** (4), H142–H144 (2009).
- [29] Li, Q., Jiang, Y.-B., Xu, H., Hersee, S., Han, S. M. Heteroepitaxy of high-quality Ge on Si by nanoscale Ge seeds grown through a thin layer of SiO₂. *Applied Physics Letters*. **85** (11), 1928–1930 (2004).
- [30] Halbwax, M. et al. Epitaxial growth of Ge on a thin SiO₂ layer by ultrahigh vacuum chemical

vapor deposition. *Journal of Crystal Growth*. **308** (1), 26–29 (2007).

[31] Leonhardt, D., Ghosh, S., Han, S. M. Origin and removal of stacking faults in Ge islands nucleated on Si within nanoscale openings in SiO₂. *Journal of Applied Physics*. **10** (7), 073516 (2011).

[32] Takada, Y., Osaka, J., Ishikawa, Y., Wada, K. Effect of Mesa Shape on Threading Dislocation Density in Ge Epitaxial Layers on Si after Post-Growth Annealing. *Japanese Journal of Applied Physics*. Part 1, **49** (4S), 04DG23 (2010).

[33] Ishikawa, Y., Wada, K. Germanium for silicon photonics. *Thin Solid Films*. **518** (6), S83–S87 (2010).

[34] Nagatomo, S., Ishikawa, Y., Hoshino, S. Near-infrared laser annealing of Ge layers epitaxially grown on Si for high-performance photonic devices. *Journal of Vacuum Science & Technology B*. **35** (5), 051206 (2017).

[35] Ayers, J. E., Schowalter, L. J., Ghandhi, S. K. Post-growth thermal annealing of GaAs on Si(001) grown by organometallic vapor phase epitaxy. *Journal of Crystal Growth*. **125** (1), 329–335 (1992).

[36] Wang, G. et al. A model of threading dislocation density in strain-relaxed Ge and GaAs epitaxial films on Si (100). *Applied Physics Letters*. **94** (10), 102115 (2009).

[37] Leonhardt, D., Ghosh, S., Han, S. M. Defects in Ge epitaxy in trench patterned SiO₂ on Si and Ge substrates. *Journal of Crystal Growth*. **335** (1), 62–65 (2011).

[38] Sammak, A., Boer, W. B., Nanver, L. K. Ge-on-Si: Single-crystal selective epitaxial growth in a CVD reactor. *ECS Transactions*. **50** (9), 507–512 (2012).

[39] Ishikawa, Y., Wada, K., Cannon, D. D., Liu, J., Luan, H.-C., Kimerling, L. C. Strain-induced band gap shrinkage in Ge grown on Si substrate. *Applied Physics Letters*. **82** (13), 2044–2046 (2003).

[40] Bolkhovityanov, Y. B., Gutakovskii, A. K., Deryabin, A. S., Sokolov, L. V. Edge Misfit Dislocations in Ge_xSi_{1-x}/Si(001) (x~1) Heterostructures: Role of Buffer Ge_ySi_{1-y} (y < x) Interlayer in Their Formation. *Physics of the Solid State*. **53** (9), 1791–1797 (2011).

[41] Bourret, A. How to control the self-organization of nanoparticles by bonded thin layers. *Surface Science*. **432** (1), 37–53 (1999).

[42] Hirth, J. P., Lothe, J. Grain boundaries, in *Theory of Dislocations*, 2nd ed. New York, NY, USA: Wiley, chapter **19**, 697–750 (1982).

[43] Mizuno, Y., Yako, M., Luan, N. M., Wada, K. Strain tuning of Ge bandgap by selective epigrowth for electro-absorption modulators, in *Proceedings of SPIE Photonics West, San Francisco, CA, USA*. **9367**, 1–6 (2015).

[44] Nam, J. H. et al. Lateral overgrowth of germanium for monolithic integration of germanium-on-insulator on silicon. *Journal of Crystal Growth*. **416** (15), 21–27 (2015).

[45] Fitch, J. T. Selectivity Mechanisms in Low Pressure Selective Epitaxial Silicon Growth. *Journal of The Electrochemical Society*. **141** (4), 1046–1055 (1994).

[46] Ye, H., Yu, J. Germanium epitaxy on silicon. *Science and Technology of Advanced Materials*. **15** (2), 1–9 (2014).

Figure 1

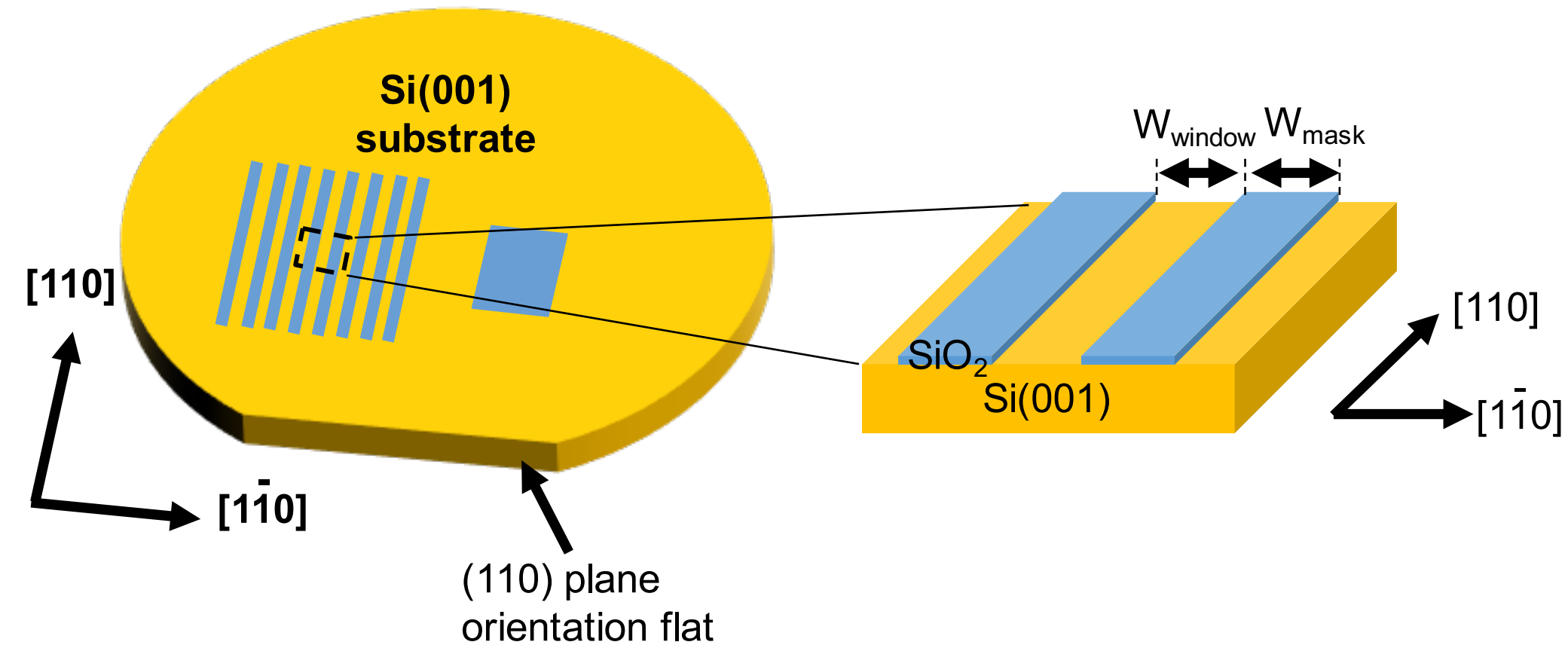
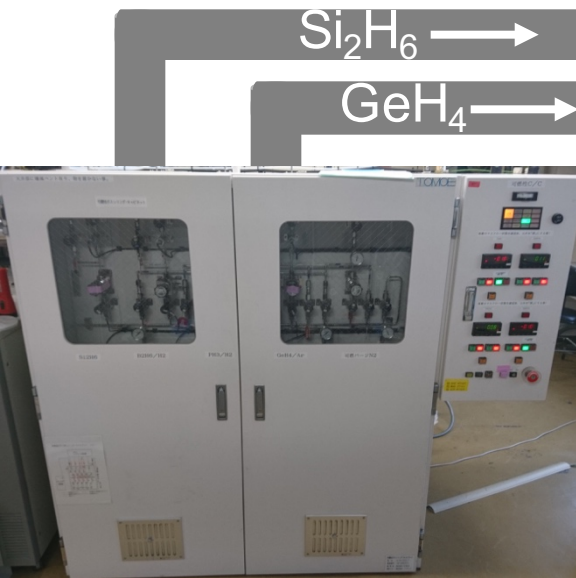


Figure 2



Gas cabinet



Growth
chamber

Load lock
chamber

Operation
panel

Figure 3

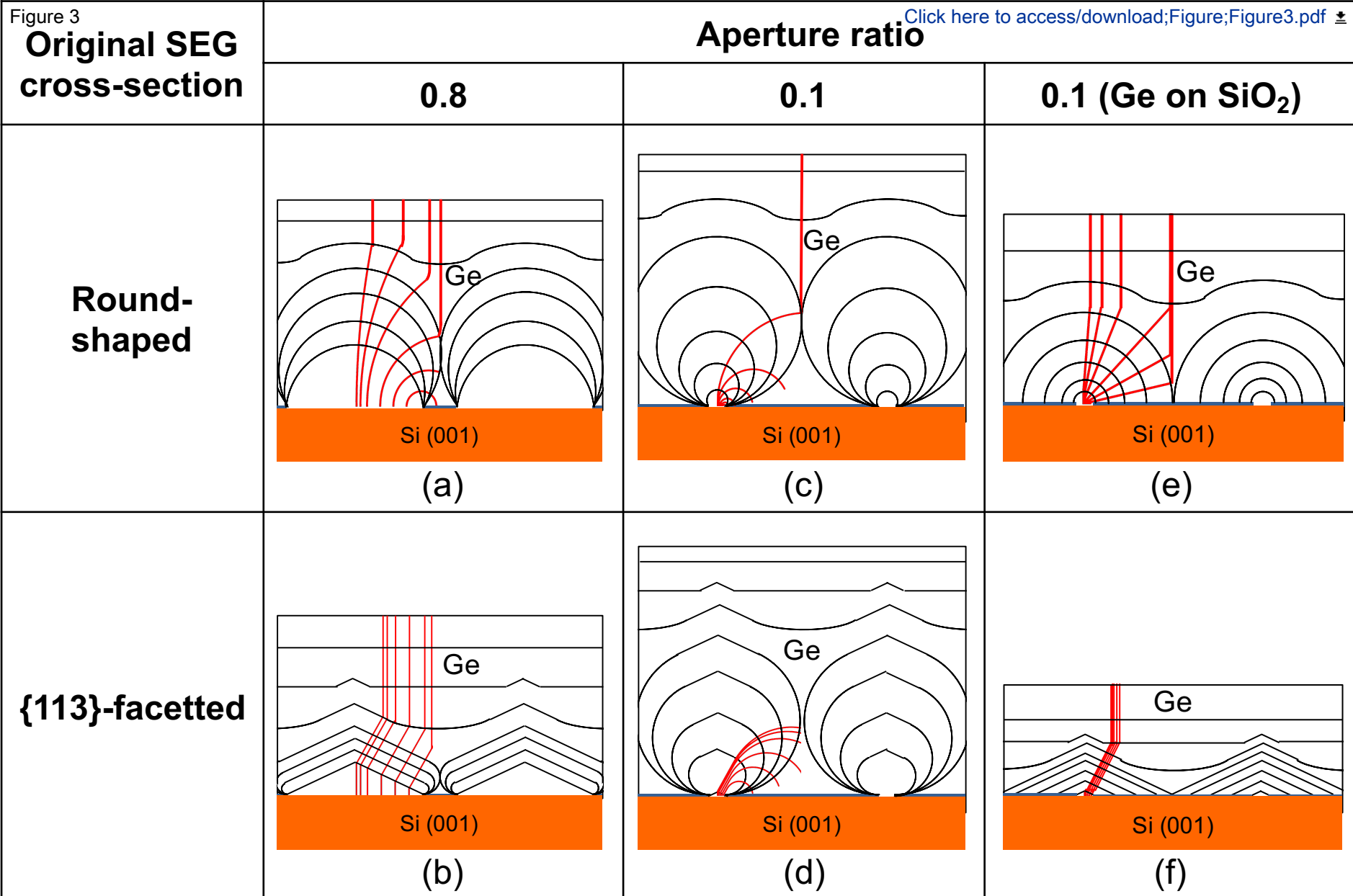


Figure 4

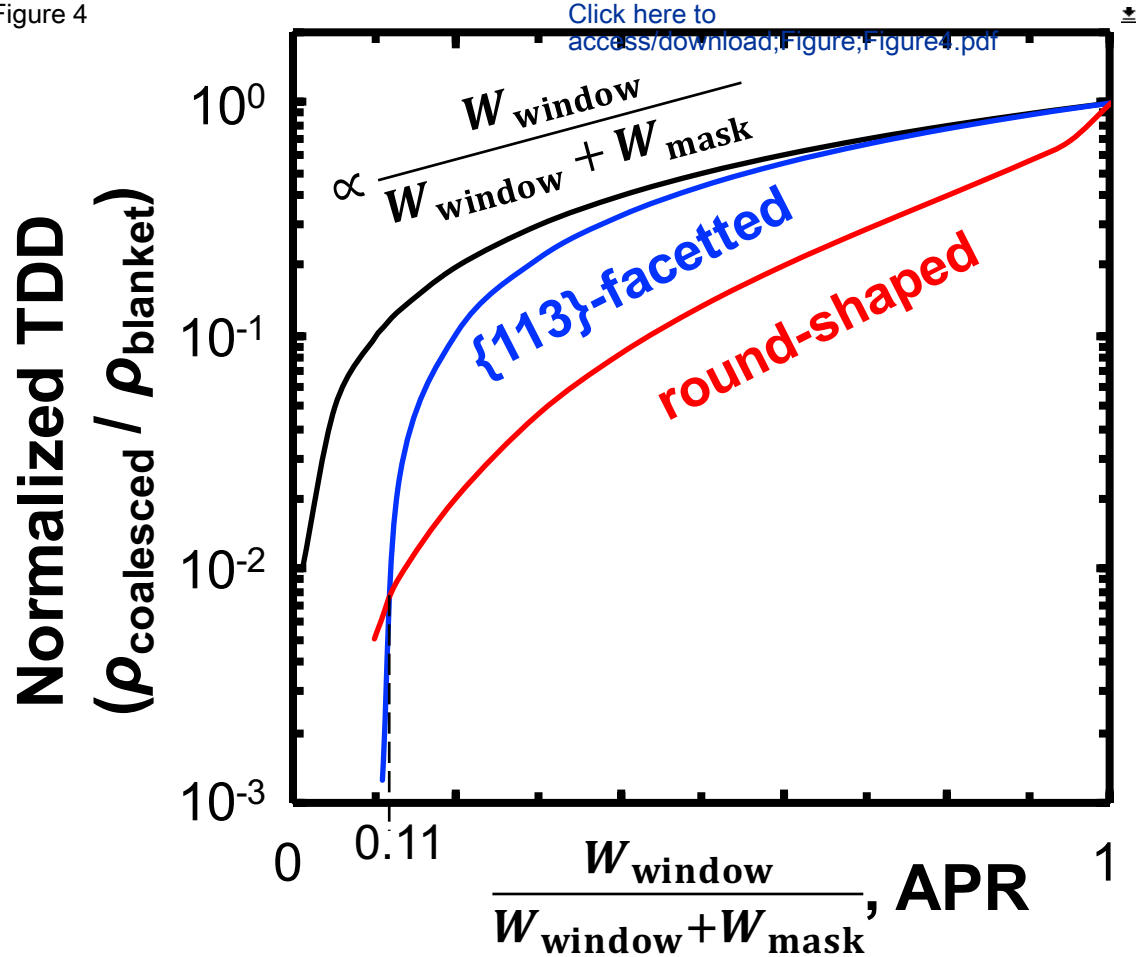


Figure 5

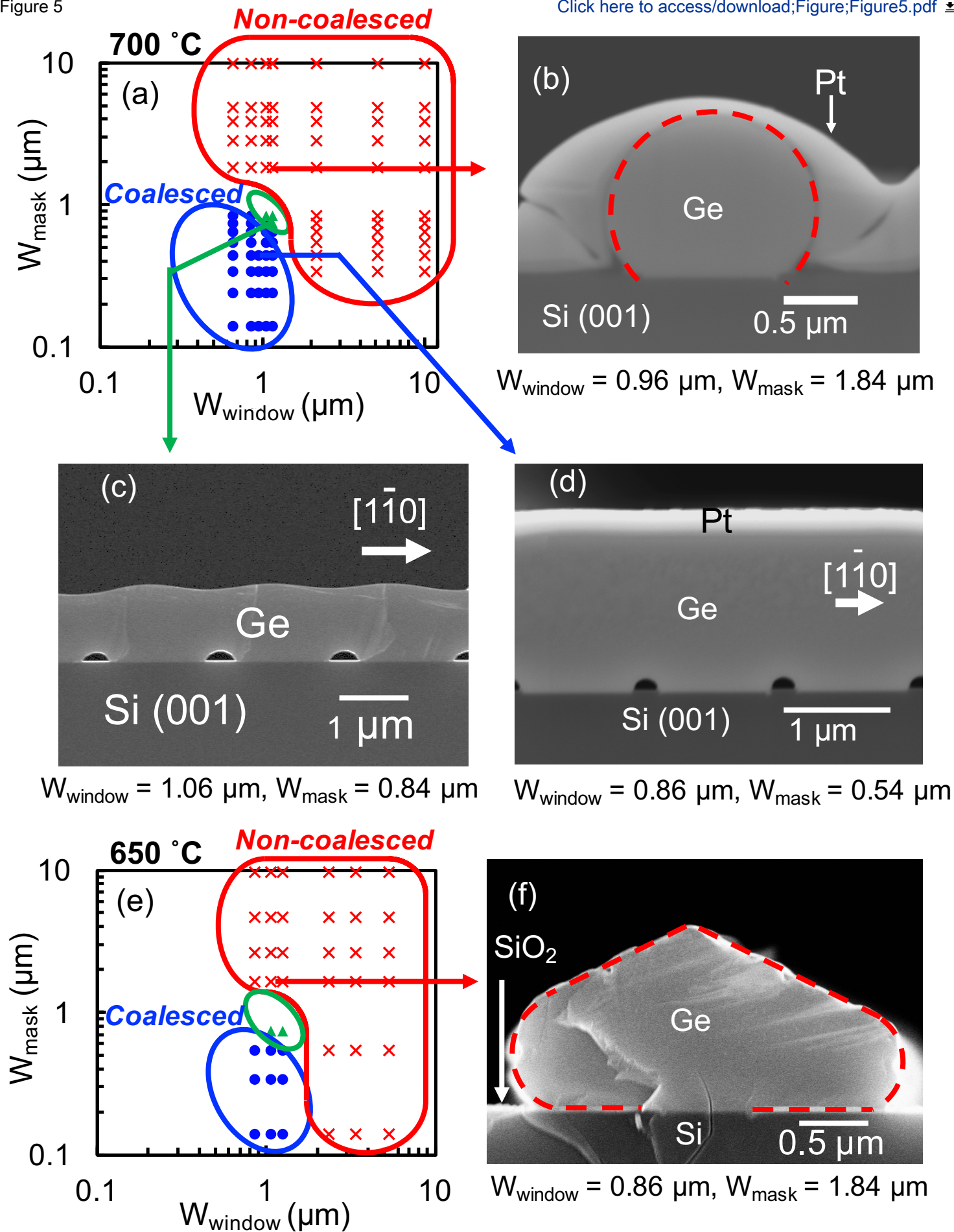
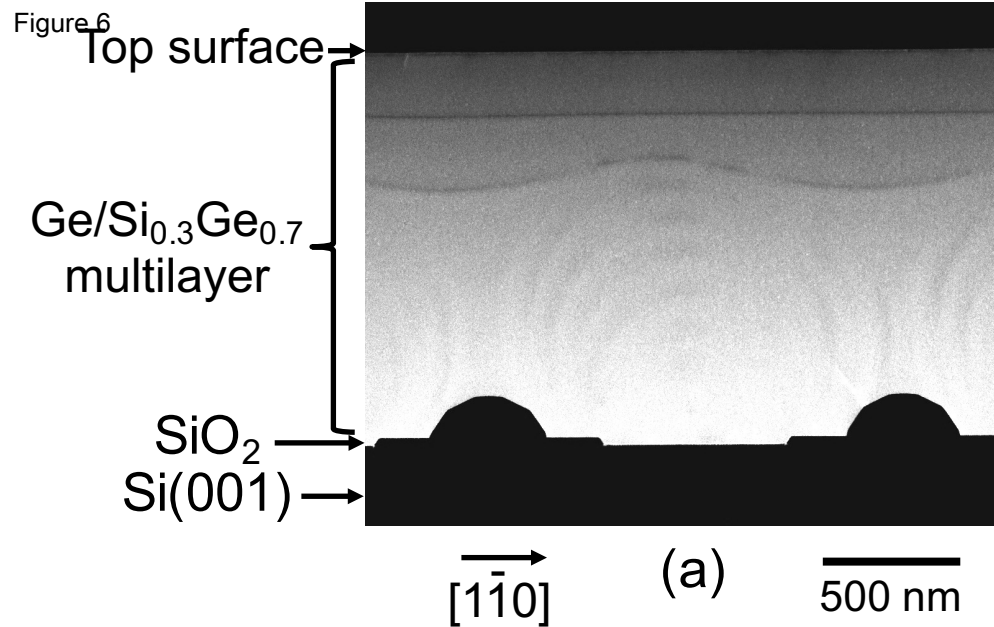
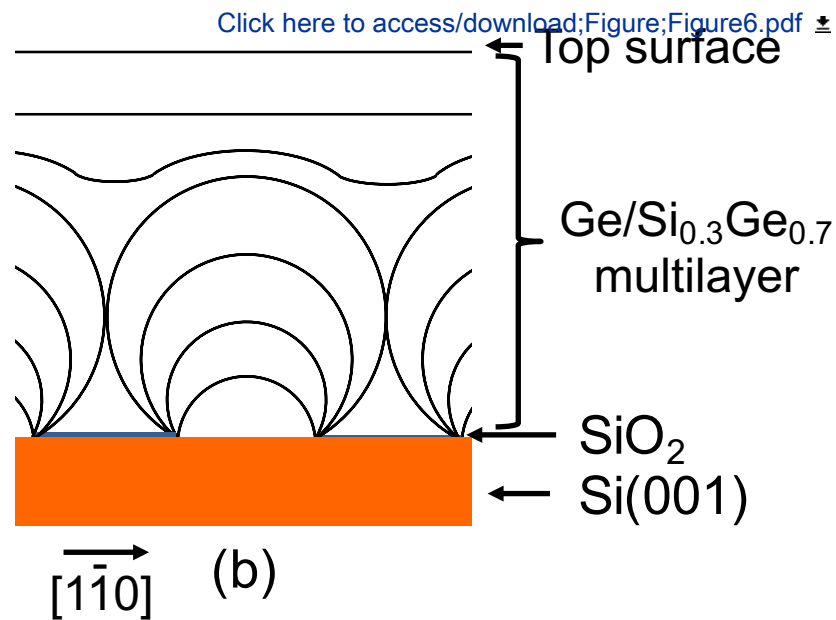
[Click here to access/download;Figure;Figure5.pdf](#)

Figure 6



[Click here to access/download;Figure;Figure6.pdf](#)



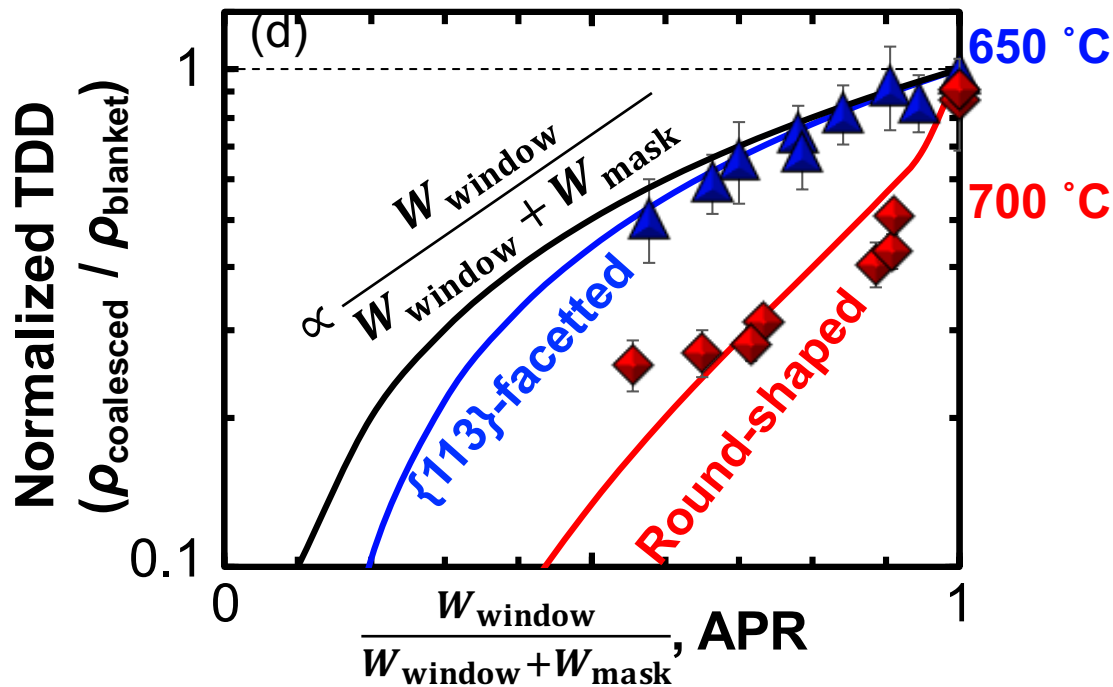
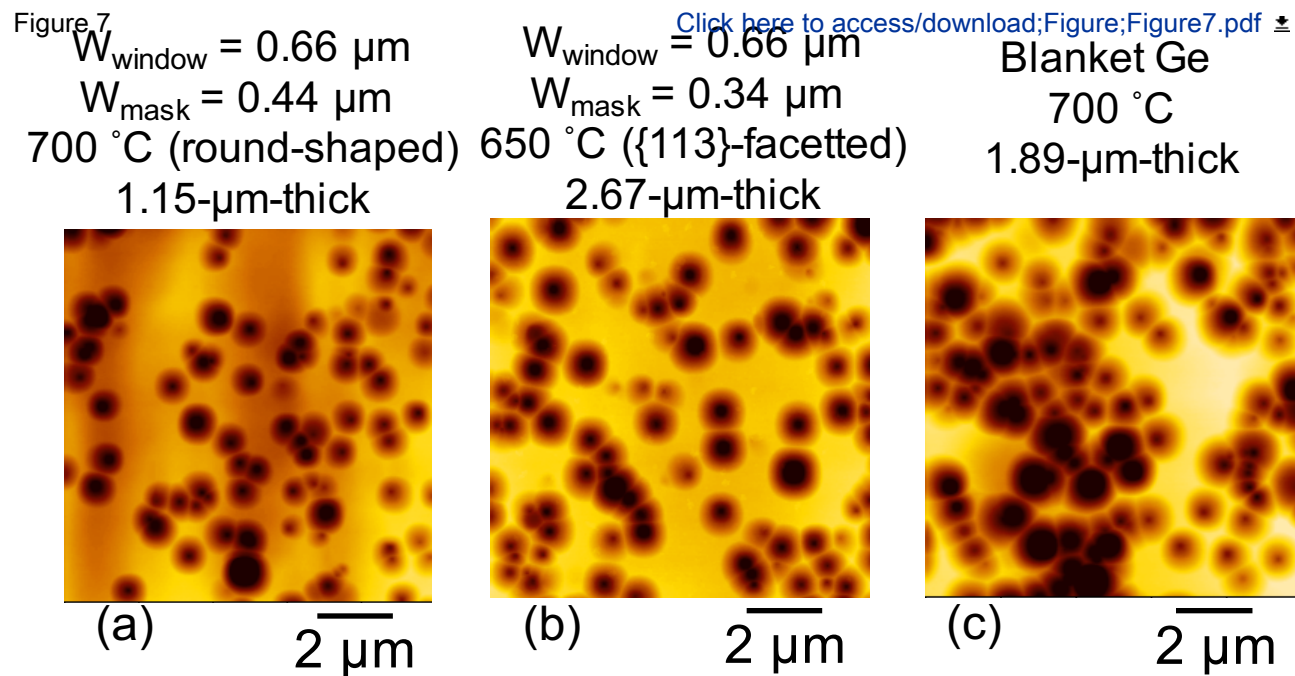
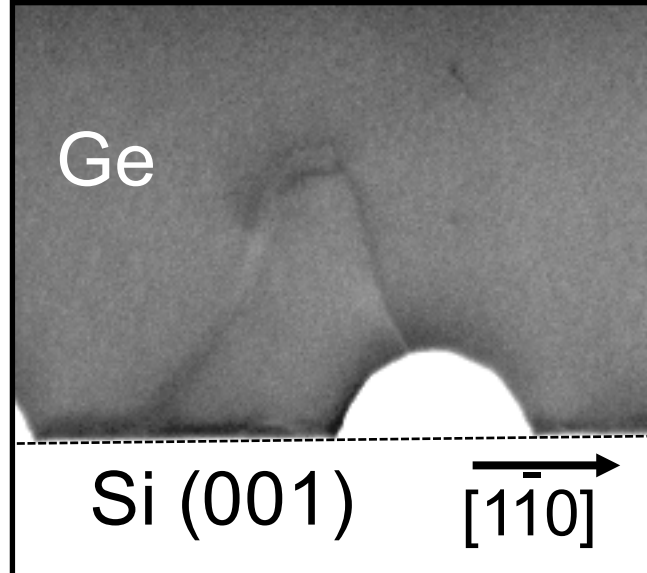
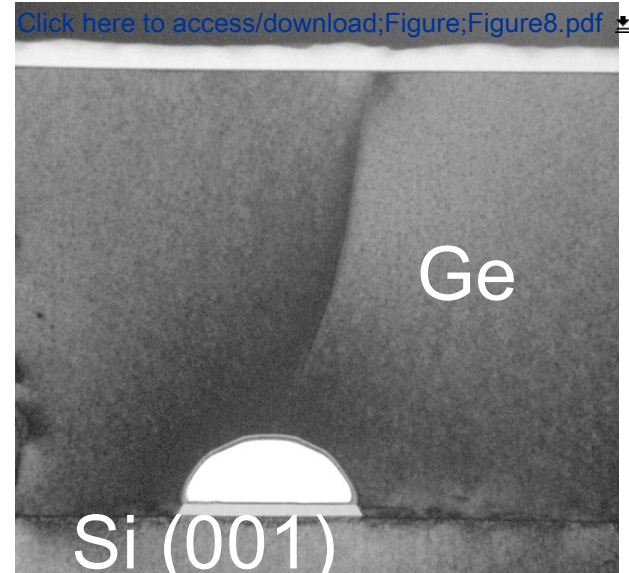


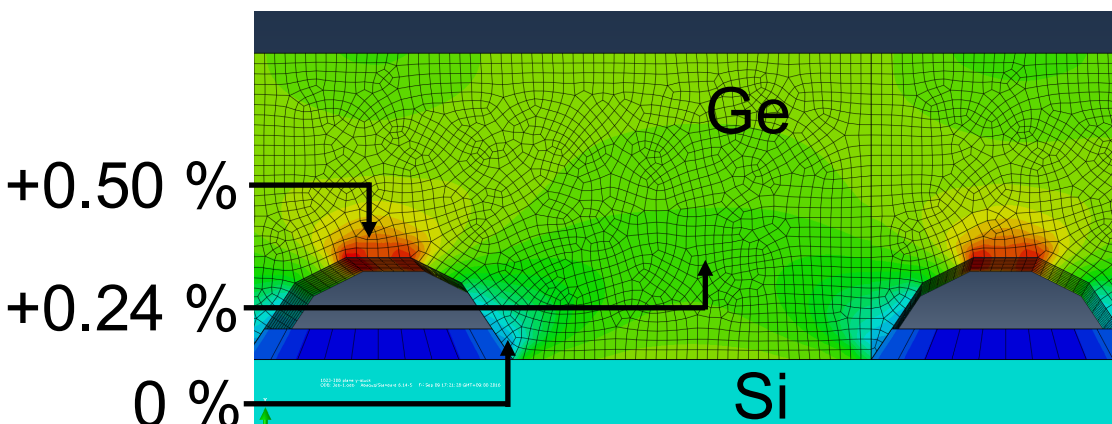
Figure 8



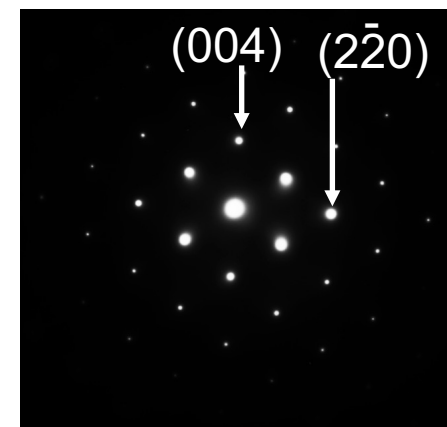
(a) 500 nm



(c) 500 nm

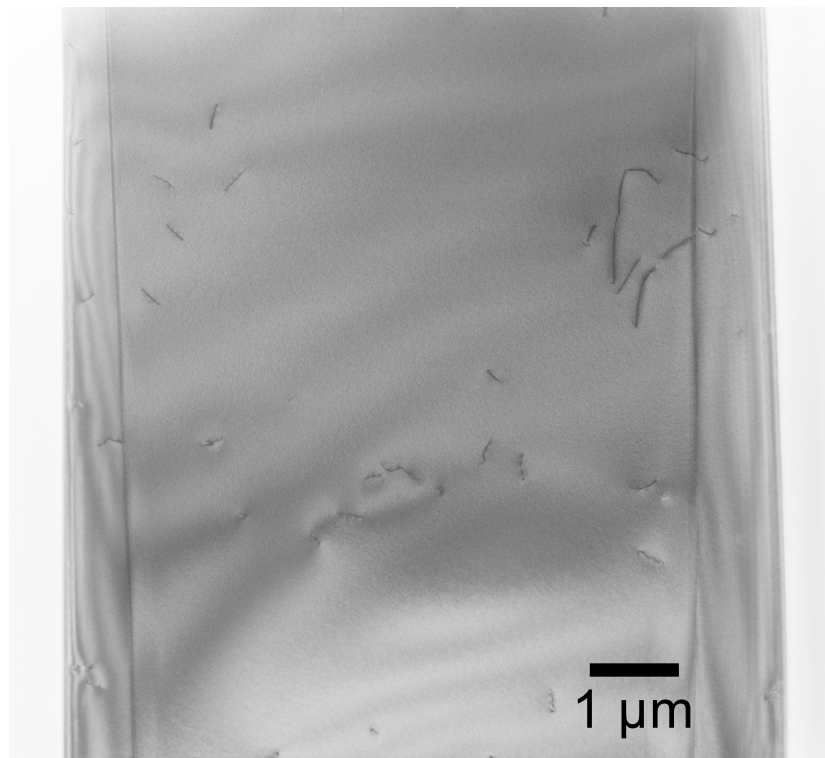
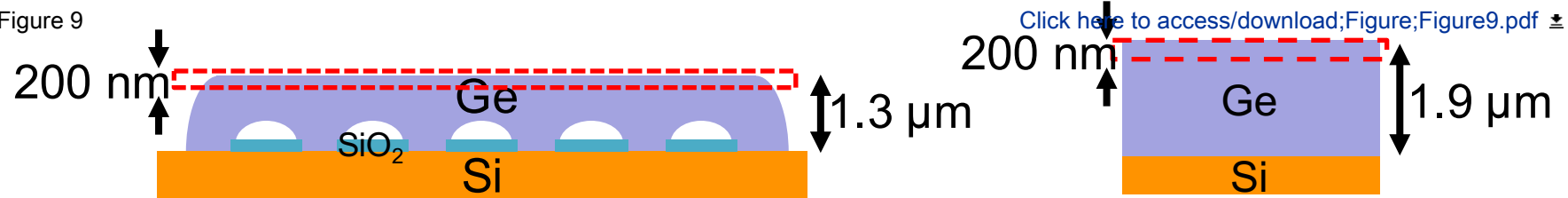


(b)

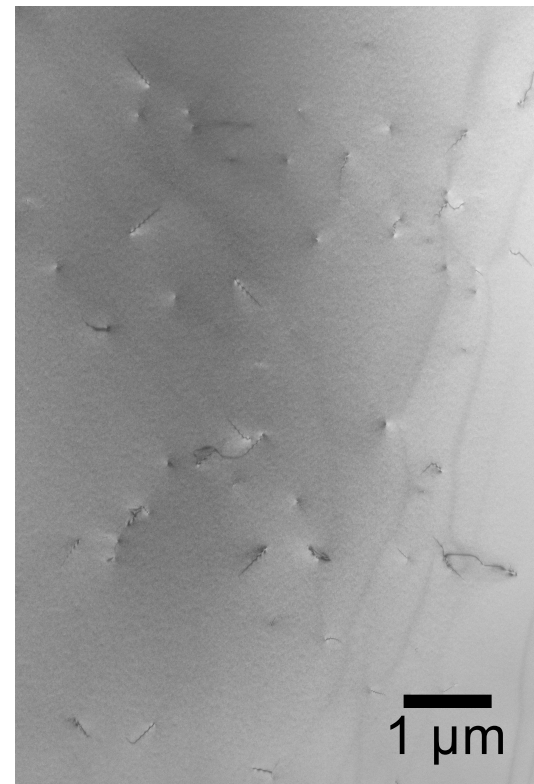


(d)

Figure 9



(a)

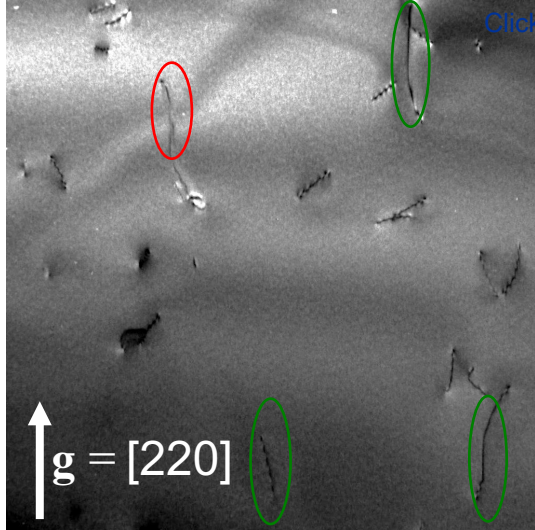


(b)

Figure 10

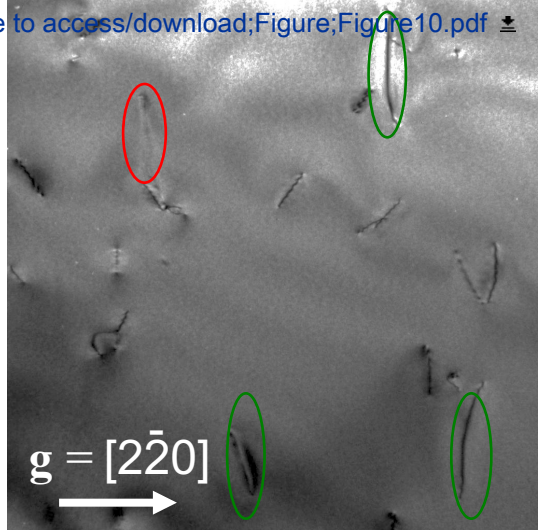
[Click here to access/download;Figure;Figure10.pdf](#)

Direction of
 SiO_2 mask stripes



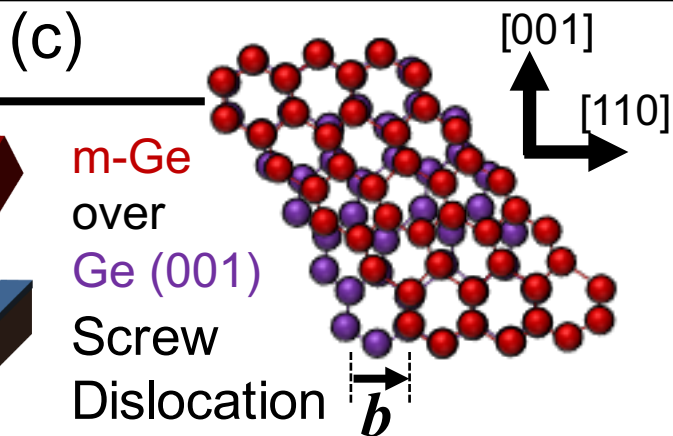
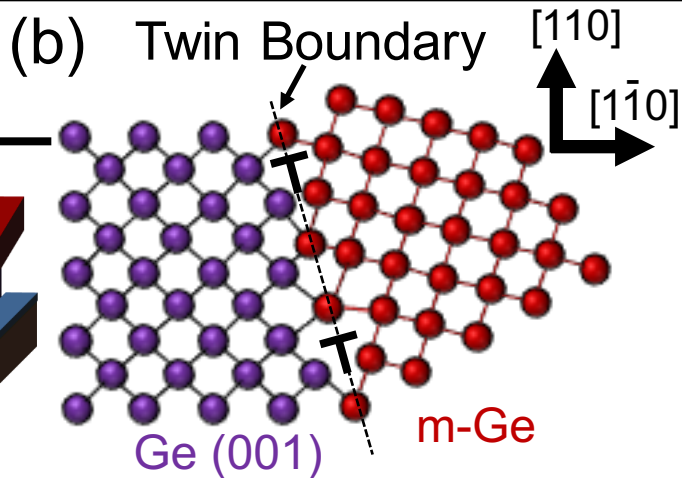
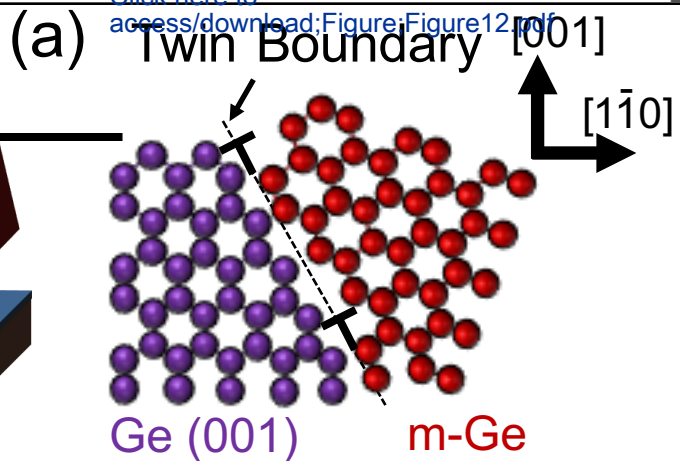
(a)

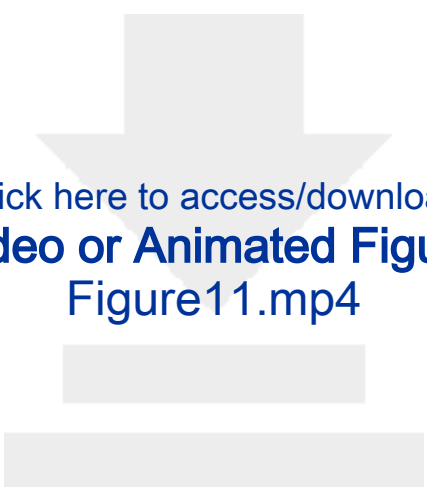
1 μm



(b)

1 μm





Click here to access/download
Video or Animated Figure
Figure11.mp4

Method	Achieved TDD (cm ⁻²)	Temperature (°C)
Thermal annealing	2e7	≈900 °C
SiGe graded buffer	1e6	growth temperature (600–700 °C)
ART	1e6	growth temperature (600–700 °C)
Si pillar seeds	1e5	≈800 °C
This work	4e7	growth temperature (700 °C)

Buffer layer thickness

≈100 nm
(low-temperature buffer)

2–3 μm

500–1000 nm

≈5 μm

≈150 nm

Name of Material/ Equipment	Company	Catalog Number	Comments/Description
AFM	SII NanoTechnology	SPI-3800N	Software for Electronics
BHF	DAIKIN	BHF-63U	
CAD design	AUTODESK	AutoCAD 2013	
CH ₃ COOH	Kanto-Kagaku	Acetic Acid	
CVD	Canon ANELVA	I-2100 SRE	
Developer	ZEON	ZED	
Developer rinse	ZEON	ZMD	
EB writer	ADVANTEST	F5112+VD01	
Furnace	Koyo Thermo System	KTF-050N-PA	
HF, 0.5 %	Kanto-Kagaku	0.5 % HF	
HF, 50 %	Kanto-Kagaku	50 % HF	for Electronics
HNO ₃ , 61 %	Kanto-Kagaku	HNO3 1.38	
I ₂	Kanto-Kagaku	Iodine 100g	
Photoresist	ZEON	ZEP520A	
Photoresist remover	Tokyo Ohka	Hakuri-104	
Surfactant	Tokyo Ohka	OAP	
TEM	JEOL	JEM-2010HC	



1 Alewife Center #200
Cambridge, MA 02140
tel. 617.945.9051
www.jove.com

ARTICLE AND VIDEO LICENSE AGREEMENT

Title of Article:	A method of dislocation reduction in Ge epitaxial layers with semicylindrical voids on Si: theoretical calculation and experimental verification
Author(s):	Motoki Yako, Yasuhiko Ishikawa, Eiji Abe, and Kazumi Wada

Item 1: The Author elects to have the Materials be made available (as described at <http://www.jove.com/publish>) via:



Standard Access



Open Access

Item 2: Please select one of the following items:



The Author is **NOT** a United States government employee.



The Author is a United States government employee and the Materials were prepared in the course of his or her duties as a United States government employee.



The Author is a United States government employee but the Materials were NOT prepared in the course of his or her duties as a United States government employee.

ARTICLE AND VIDEO LICENSE AGREEMENT

1. **Defined Terms.** As used in this Article and Video License Agreement, the following terms shall have the following meanings: **"Agreement"** means this Article and Video License Agreement; **"Article"** means the article specified on the last page of this Agreement, including any associated materials such as texts, figures, tables, artwork, abstracts, or summaries contained therein; **"Author"** means the author who is a signatory to this Agreement; **"Collective Work"** means a work, such as a periodical issue, anthology or encyclopedia, in which the Materials in their entirety in unmodified form, along with a number of other contributions, constituting separate and independent works in themselves, are assembled into a collective whole; **"CRC License"** means the Creative Commons Attribution-Non Commercial-No Derivs 3.0 Unported Agreement, the terms and conditions of which can be found at: <http://creativecommons.org/licenses/by-nc-nd/3.0/legalcode>; **"Derivative Work"** means a work based upon the Materials or upon the Materials and other pre-existing works, such as a translation, musical arrangement, dramatization, fictionalization, motion picture version, sound recording, art reproduction, abridgment, condensation, or any other form in which the Materials may be recast, transformed, or adapted; **"Institution"** means the institution, listed on the last page of this Agreement, by which the Author was employed at the time of the creation of the Materials; **"JoVE"** means MyJoVE Corporation, a Massachusetts corporation and the publisher of The Journal of Visualized Experiments; **"Materials"** means the Article and / or the Video; **"Parties"** means the Author and JoVE; **"Video"** means any video(s) made by the Author, alone or in conjunction with any other parties, or by JoVE or its affiliates or agents, individually or in collaboration with the Author or any other parties, incorporating all or any portion

of the Article, and in which the Author may or may not appear.

2. **Background.** The Author, who is the author of the Article, in order to ensure the dissemination and protection of the Article, desires to have the JoVE publish the Article and create and transmit videos based on the Article. In furtherance of such goals, the Parties desire to memorialize in this Agreement the respective rights of each Party in and to the Article and the Video.

3. **Grant of Rights in Article.** In consideration of JoVE agreeing to publish the Article, the Author hereby grants to JoVE, subject to **Sections 4** and **7** below, the exclusive, royalty-free, perpetual (for the full term of copyright in the Article, including any extensions thereto) license (a) to publish, reproduce, distribute, display and store the Article in all forms, formats and media whether now known or hereafter developed (including without limitation in print, digital and electronic form) throughout the world, (b) to translate the Article into other languages, create adaptations, summaries or extracts of the Article or other Derivative Works (including, without limitation, the Video) or Collective Works based on all or any portion of the Article and exercise all of the rights set forth in (a) above in such translations, adaptations, summaries, extracts, Derivative Works or Collective Works and (c) to license others to do any or all of the above. The foregoing rights may be exercised in all media and formats, whether now known or hereafter devised, and include the right to make such modifications as are technically necessary to exercise the rights in other media and formats. If the "Open Access" box has been checked in **Item 1** above, JoVE and the Author hereby grant to the public all such rights in the Article as provided in, but subject to all limitations and requirements set forth in, the CRC License.

ARTICLE AND VIDEO LICENSE AGREEMENT

4. **Retention of Rights in Article.** Notwithstanding the exclusive license granted to JoVE in **Section 3** above, the Author shall, with respect to the Article, retain the non-exclusive right to use all or part of the Article for the non-commercial purpose of giving lectures, presentations or teaching classes, and to post a copy of the Article on the Institution's website or the Author's personal website, in each case provided that a link to the Article on the JoVE website is provided and notice of JoVE's copyright in the Article is included. All non-copyright intellectual property rights in and to the Article, such as patent rights, shall remain with the Author.

5. **Grant of Rights in Video – Standard Access.** This **Section 5** applies if the "Standard Access" box has been checked in **Item 1** above or if no box has been checked in **Item 1** above. In consideration of JoVE agreeing to produce, display or otherwise assist with the Video, the Author hereby acknowledges and agrees that, Subject to **Section 7** below, JoVE is and shall be the sole and exclusive owner of all rights of any nature, including, without limitation, all copyrights, in and to the Video. To the extent that, by law, the Author is deemed, now or at any time in the future, to have any rights of any nature in or to the Video, the Author hereby disclaims all such rights and transfers all such rights to JoVE.

6. **Grant of Rights in Video – Open Access.** This **Section 6** applies only if the "Open Access" box has been checked in **Item 1** above. In consideration of JoVE agreeing to produce, display or otherwise assist with the Video, the Author hereby grants to JoVE, subject to **Section 7** below, the exclusive, royalty-free, perpetual (for the full term of copyright in the Article, including any extensions thereto) license (a) to publish, reproduce, distribute, display and store the Video in all forms, formats and media whether now known or hereafter developed (including without limitation in print, digital and electronic form) throughout the world, (b) to translate the Video into other languages, create adaptations, summaries or extracts of the Video or other Derivative Works or Collective Works based on all or any portion of the Video and exercise all of the rights set forth in (a) above in such translations, adaptations, summaries, extracts, Derivative Works or Collective Works and (c) to license others to do any or all of the above. The foregoing rights may be exercised in all media and formats, whether now known or hereafter devised, and include the right to make such modifications as are technically necessary to exercise the rights in other media and formats. For any Video to which this **Section 6** is applicable, JoVE and the Author hereby grant to the public all such rights in the Video as provided in, but subject to all limitations and requirements set forth in, the CRC License.

7. **Government Employees.** If the Author is a United States government employee and the Article was prepared in the course of his or her duties as a United States government employee, as indicated in **Item 2** above, and any of the licenses or grants granted by the Author hereunder exceed the scope of the 17 U.S.C. 403, then the rights granted hereunder shall be limited to the maximum

rights permitted under such statute. In such case, all provisions contained herein that are not in conflict with such statute shall remain in full force and effect, and all provisions contained herein that do so conflict shall be deemed to be amended so as to provide to JoVE the maximum rights permissible within such statute.

8. **Protection of the Work.** The Author(s) authorize JoVE to take steps in the Author(s) name and on their behalf if JoVE believes some third party could be infringing or might infringe the copyright of either the Author's Article and/or Video.

9. **Likeness, Privacy, Personality.** The Author hereby grants JoVE the right to use the Author's name, voice, likeness, picture, photograph, image, biography and performance in any way, commercial or otherwise, in connection with the Materials and the sale, promotion and distribution thereof. The Author hereby waives any and all rights he or she may have, relating to his or her appearance in the Video or otherwise relating to the Materials, under all applicable privacy, likeness, personality or similar laws.

10. **Author Warranties.** The Author represents and warrants that the Article is original, that it has not been published, that the copyright interest is owned by the Author (or, if more than one author is listed at the beginning of this Agreement, by such authors collectively) and has not been assigned, licensed, or otherwise transferred to any other party. The Author represents and warrants that the author(s) listed at the top of this Agreement are the only authors of the Materials. If more than one author is listed at the top of this Agreement and if any such author has not entered into a separate Article and Video License Agreement with JoVE relating to the Materials, the Author represents and warrants that the Author has been authorized by each of the other such authors to execute this Agreement on his or her behalf and to bind him or her with respect to the terms of this Agreement as if each of them had been a party hereto as an Author. The Author warrants that the use, reproduction, distribution, public or private performance or display, and/or modification of all or any portion of the Materials does not and will not violate, infringe and/or misappropriate the patent, trademark, intellectual property or other rights of any third party. The Author represents and warrants that it has and will continue to comply with all government, institutional and other regulations, including, without limitation all institutional, laboratory, hospital, ethical, human and animal treatment, privacy, and all other rules, regulations, laws, procedures or guidelines, applicable to the Materials, and that all research involving human and animal subjects has been approved by the Author's relevant institutional review board.

11. **JoVE Discretion.** If the Author requests the assistance of JoVE in producing the Video in the Author's facility, the Author shall ensure that the presence of JoVE employees, agents or independent contractors is in accordance with the relevant regulations of the Author's institution. If more than one author is listed at the beginning of this Agreement, JoVE may, in its sole

ARTICLE AND VIDEO LICENSE AGREEMENT

discretion, elect not take any action with respect to the Article until such time as it has received complete, executed Article and Video License Agreements from each such author. JoVE reserves the right, in its absolute and sole discretion and without giving any reason therefore, to accept or decline any work submitted to JoVE. JoVE and its employees, agents and independent contractors shall have full, unfettered access to the facilities of the Author or of the Author's institution as necessary to make the Video, whether actually published or not. JoVE has sole discretion as to the method of making and publishing the Materials, including, without limitation, to all decisions regarding editing, lighting, filming, timing of publication, if any, length, quality, content and the like.

12. **Indemnification.** The Author agrees to indemnify JoVE and/or its successors and assigns from and against any and all claims, costs, and expenses, including attorney's fees, arising out of any breach of any warranty or other representations contained herein. The Author further agrees to indemnify and hold harmless JoVE from and against any and all claims, costs, and expenses, including attorney's fees, resulting from the breach by the Author of any representation or warranty contained herein or from allegations or instances of violation of intellectual property rights, damage to the Author's or the Author's institution's facilities, fraud, libel, defamation, research, equipment, experiments, property damage, personal injury, violations of institutional, laboratory, hospital, ethical, human and animal treatment, privacy or other rules, regulations, laws, procedures or guidelines, liabilities and other losses or damages related in any way to the submission of work to JoVE, making of videos by JoVE, or publication in JoVE or elsewhere by JoVE. The Author shall be responsible for, and shall hold JoVE harmless from, damages caused by lack of sterilization, lack of cleanliness or by contamination due to


the making of a video by JoVE its employees, agents or independent contractors. All sterilization, cleanliness or decontamination procedures shall be solely the responsibility of the Author and shall be undertaken at the Author's expense. All indemnifications provided herein shall include JoVE's attorney's fees and costs related to said losses or damages. Such indemnification and holding harmless shall include such losses or damages incurred by, or in connection with, acts or omissions of JoVE, its employees, agents or independent contractors.

13. **Fees.** To cover the cost incurred for publication, JoVE must receive payment before production and publication the Materials. Payment is due in 21 days of invoice. Should the Materials not be published due to an editorial or production decision, these funds will be returned to the Author. Withdrawal by the Author of any submitted Materials after final peer review approval will result in a US\$1,200 fee to cover pre-production expenses incurred by JoVE. If payment is not received by the completion of filming, production and publication of the Materials will be suspended until payment is received.

14. **Transfer, Governing Law.** This Agreement may be assigned by JoVE and shall inure to the benefits of any of JoVE's successors and assignees. This Agreement shall be governed and construed by the internal laws of the Commonwealth of Massachusetts without giving effect to any conflict of law provision thereunder. This Agreement may be executed in counterparts, each of which shall be deemed an original, but all of which together shall be deemed to be one and the same agreement. A signed copy of this Agreement delivered by facsimile, e-mail or other means of electronic transmission shall be deemed to have the same legal effect as delivery of an original signed copy of this Agreement.

A signed copy of this document must be sent with all new submissions. Only one Agreement is required per submission.

CORRESPONDING AUTHOR

Name:	Kazumi Wada	
Department:	Department of Materials Science and Engineering	
Institution:	Massachusetts Institute of Technology and University of Tokyo	
Title:	Visiting Professor and Emeritus Professor	
Signature:		Date: Nov. 21, '18

Please submit a **signed and dated** copy of this license by one of the following three methods:

1. Upload an electronic version on the JoVE submission site
2. Fax the document to +1.866.381.2236
3. Mail the document to JoVE / Attn: JoVE Editorial / 1 Alewife Center #200 / Cambridge, MA 02140

Reply to the Reviewer

We would like to thank the reviewers for their fruitful comments. Since Reviewer #1 and #2 suggests that the original manuscript is suitable for publication, we would like to answer Reviewer #3's comments. Considering their comments, we have revised the manuscript and prepared a manuscript for reviewers with highlight. In the revised manuscript for review, the revised/added descriptions are highlighted by **BLUE** characters.

Reviewer #3

[General Comment]

The authors suggest a method of dislocation reduction in Ge epitaxial layers with semicylindrical voids on Si. they suggest a theoretical calculation and experimental verification

I suggest to give the manuscript back to the authors in order to revise it:

Major Concerns:

We are assessing a manuscript for the production of a movie, so the following things are disturbing the reviewers assessment "ab initio"

[Comment 1]

The manuscript - 34 pages - in the present shape is hard to assess since many figures are presented

- (a) at the end of the manuscript
- (b) not enumerated in their original order
- (c) without captions

You cannot jump back and forth in a movie either....

[Reply 1]

We have prepared a manuscript for reviewer, which is modified for easy reading.

Here, we put the figures where they are mentioned.

We are afraid there were some mistakes in uploading the movies in the last submission.

We believe now you can jump back and forth in the movies.

[Comment 2]

The intro of the manuscript proposal lacks the definition of clear merits; the "eye catcher" is missing

[Reply 2]

We have added a sentence to mention the merit of this method at the end of INTRODUCTION part (lines 98–100) and in DISCUSSION PART (lines 585–593).

The merit of the proposed method is that dislocations are removed without any thermal annealing or thick buffer layers.

Conventional methods have been employed thermal annealing or thick buffer layer as

mentioned in lines 67–81 in INTRODUCTION and Table 1 in DISCUSSION.

[Comment 3]

The subject of presented work should profit from the presentation as a movie as compared as to be published as a methods paper in some materials journal or applied physics journal

So.. I am missing in the presentation of the manuscript any initial trial

(a) of presenting the procedure in the laboratory

(b) of presenting something "dynamical" which is

(*) interesting enough to be directly followed by the consumers eye

(*) which is easy enough to be understood at first or second sight

I do not see the sense of the animated figures as such, without a direct and immediate counterpart as the demonstration in situ would be.

[Reply 3]

We have revised the PROTOCOL part in order to show more details of experimental procedure.

The revised PROTOCOL part shows detailed procedure in the laboratory so that anyone can understand/reproduce the experiments.

[Comment 4]

The manuscript so far lacks in one sense coherence:

A movie should be interesting for an increased auditorium; it should be understandable for deaf as well as for blind people with some efforts! It should also be interesting for non-experts such as students in the advanced classes

[Reply 4]

As the reviewer pointed out, this manuscript would be somehow difficult to understand for non-experts because the presented method employs a new mechanism (image force) to reduce TDD in Ge: even experts of Ge growth on Si are not familiar with image force.

However, the basic idea, TDs are bent to be normal to growth surface, is so simple that everyone can understand what happens in Ge if one can understand geometrical structure.

Thus, we have added schematic illustrations (Fig. 3 in the revised manuscript) in order to help understanding of geometrical structure of SEG masks.

[Comment 5]

A method publishing manuscript must be assessible for reproduction

[Reply 5]

We have revised PROTOCOL part in order to show more details of experimental procedure.

[Comment 6]

A method publishing manuscript must be embedded in the research background as the reader, or the auditorium must see bright and clear why it should be an advantage to use the method,

compared to others, what is the improvement, bright and clear in figures words and numbers.

The manuscript should start with this as an intro and it should praise the merits again in the discussion.

[Reply 6]

We have added a description showing the advantage of this method at the end of INTRODUCTION part (lines 98–100) and in DISCUSSION PART (lines 585–593).

In DISCUSSION part, we have added a table showing the summary of conventional/presented TDD reduction methods in order to make the advantage of the presented method clear.

[Comment 7]

The geometry aspects of this manuscript:

This aspect naturally includes many aspects where the crystal geometry plays a role and the application of geometrical, spacial techniques. My personal spacial sense is beyond doubt above average in the community of physicists and christallographers. If I need to read a technical passage many times, or if I have to repeat an animated figure a few times, and I still do not see their claimed to be key feature, it will not appeal to the broad mass of material scientists and in needs to be improved.

Actually so far I do not see these points presented well in this manuscript. For these reasons I suggest to give the manuscript back for revision to the authors.

[Reply 7]

Although we would not fully understand exact meaning of your comment, we have regarded your “Comment 7” that our previous manuscript was not so clear and it was difficult to understand geometrical structure.

In order to help geometrical understanding, we have added a figure (Fig. 3 in the revised manuscript) showing schematic illustrations of SEG masks on a Si(001) substrate.

We believe that everybody sees Fig. 3 can understand the geometrical structure of SEG masks used in the present work, and we could answer your “Comment 7”.

Rebuttal Letter

Title: A method of dislocation reduction in Ge epitaxial layers with semicylindrical voids on Si: theoretical calculation and experimental verification

Submission number: JoVE58897

Dear Dr. Vineeta Bajaj,
Review Editor of JoVE,

We are grateful to submit our manuscript to JoVE, entitled “A method of dislocation reduction in Ge epitaxial layers with semicylindrical voids on Si: theoretical calculation and experimental verification.”

We have revised our manuscript in response to your comments as follows.

[Comment]

Parts of the manuscript have significant textual overlap with previous publication(s), including, possibly, the authors' own. All text must be original. Please see the attached iThenticate report and revise the following: 175-193, 199-206, 208-213, 215-224, 298-300, 304-310, 324-328, 341-344, 348-358, 360-367.

[Reply]

We have thoroughly revised the parts of the manuscript you pointed out.

The text in the revised manuscript should have no overlap with previous publications.

[Comment]

The protocol is not written as per the journal's style. Please format the manuscript accordingly. Attaching the authors instruction for your consideration.

The Protocol should be made up almost entirely of discrete steps without large paragraphs of text.

The Protocol should contain only action items that direct the reader to do something. Please number the Protocol to follow the JoVE Instructions for Authors. For example, 1 should be followed by 1.1 and then 1.1.1 and 1.1.2 if necessary.

[Reply]

We have revised the Protocol section to follow the JoVE Instruction for Authors.

Now the Protocol is made up of section 1 (1.1–1.4) and 2 (2.1.1–2.4.4).

[Comment]

Please ensure that all text in the protocol section is written in the imperative tense as if telling someone how to do the technique (e.g., “Do this,” “Ensure that,” etc.). The actions should be described in the imperative tense in complete sentences wherever possible. Avoid usage of phrases such as “could be,” “should be,” and “would be” throughout the Protocol. Any text that cannot be written in the imperative tense may be added as a “Note.”

However, notes should be concise and used sparingly. Please include all safety procedures.

[Reply]

We have revised the Protocol, and now all sentences in the revised Protocol section are written in the imperative tense.

In addition, the Protocol has been revised not to use could/should/would.

[Comment]

Please highlight 2.75 pages or less of the Protocol (including headings and spacing) that identifies the essential steps of the protocol for the video, i.e., the steps that should be visualized to tell the most cohesive story of the Protocol. The highlighted steps should form a cohesive narrative with a logical flow from one highlighted step to the next. Remember that non-highlighted Protocol steps will remain in the manuscript, and therefore will still be available to the reader.

[Reply]

Since our protocol is less than 2.75 pages (almost 2 pages), we did not highlight the manuscript.

We hope all sentences in Protocol will be shown in video because all steps are essential to our experiments.

[Comment]

Please obtain explicit copyright permission to reuse any figures from a previous publication. Explicit permission can be expressed in the form of a letter from the editor or a link to the editorial policy that allows re-prints. Please upload this information as a .doc or .docx file to your Editorial Manager account. The Figure must be cited appropriately in the Figure Legend, i.e. "This figure has been modified from [citation]."

[Reply]

We obtained permission to re-use the Figures from our previous publication, *IEEE J. Sel. Top. Quant. Elect.*, 24-6, 8201007, 2018.

We have added the citation in the corresponding Figure legends (Figs. 9, 11, 12, and 13).

[Comment]

As we are a methods journal, please revise the Discussion to explicitly cover the following in detail in 3-6 paragraphs with citations:

- a) Critical steps within the protocol
- b) Any modifications and troubleshooting of the technique
- c) Any limitations of the technique
- d) The significance with respect to existing methods
- e) Any future applications of the technique

[Reply]

We have revised Discussion part to cover a)–e) above.

The revised Discussion is made up of 3 parts; (A), (B), and (C).

(A) describes possible ways for further reduction of TDDs, corresponding to a), c), and e)

(B) describes possible ways to avoid Ge growth on SiO₂, corresponding to b) and c) and,

(C) describes suppression of TD generation when SEG Ge layers coalesce, corresponding to b).

Thank you again for your kind support and consideration on our submission to JoVE.

Sincerely,

Motoki Yako

Ph.D. candidate
Department of Materials Engineering
University of Tokyo

Copyright permission

In order to reuse previously published figures in JoVE articles, we have obtained copyright permission from IEEE (Institute of Electrical and Electronics Engineers) for the reference [20] in the revised manuscript.

[20] Yako, M., Ishikawa, Y., Abe, E., Wada, K., Defects and Their Reduction in Ge Selective Epitaxy and Coalescence Layer on Si With Semicylindrical Voids on SiO₂ Masks, *IEEE Journal of Selected Topics in Quantum Electronics*, 24 (6), 8201007 (2018).

Basic information of the license is:

License Number: 4458660728450

License date: Oct. 30, 2018

Licensed Content Publication: Selected Topics in Quantum Electronics, IEEE Journal of

License Content Title: Defects and Their Reduction in Ge Selective Epitaxy and Coalescence Layer on Si With Semicylindrical Voids on SiO₂ Masks

License Content Author: Motoki Yako

Publication the new article is in: Journal of Visualized Experiments

As the copyright permission was issued on a webpage, we attached the webpage from the next page.

**IEEE LICENSE
TERMS AND CONDITIONS**

Jan 30, 2019

This Agreement between The University of Tokyo -- Motoki Yako ("You") and IEEE ("IEEE") consists of your license details and the terms and conditions provided by IEEE and Copyright Clearance Center.

License Number	4458660728450
License date	Oct 30, 2018
Licensed Content Publisher	IEEE
Licensed Content Publication	Selected Topics in Quantum Electronics, IEEE Journal of
Licensed Content Title	Defects and Their Reduction in Ge Selective Epitaxy and Coalescence Layer on Si With Semicylindrical Voids on SiO ₂ Masks
Licensed Content Author	Motoki Yako
Licensed Content Date	Nov.-Dec. 2018
Licensed Content Volume	24
Licensed Content Issue	6
Volume number	24
Issue number	6
Type of Use	Journal/Magazine
Requestor type	commercial/for-profit
I am an IEEE member OR the author of this IEEE content.	author
IEEE Member ID	1
Format	electronic
Portion	figures/tables/graphs
Number of figures/tables/graphs	7
Figures/tables/graphs to be used	Figure 2, Figure 3(b), Figure 4(b), Figure 4(c), Figure 6, Figure 7, Figure 8
In the following language(s)	Original language
Order reference number	
Title of the article	A method of dislocation reduction in Ge epitaxial layers with semicylindrical voids on Si: theoretical calculation and experimental verification
Publication the new article is in	Journal of Visualized Experiments
Publisher of the article	JoVE
Author of new article	Motoki Yako, Yasuhiko Ishikawa, Eiji Abe, and Kazumi Wada

Expected publication date	Mar 2019
Estimated size of the article (pages)	10
Requestor Location	The University of Tokyo Rm. 334, Eng. Bldg. 4 7-3-1, Hongo Bunkyo-ku, Tokyo 113-8656 Japan Attn: The University of Tokyo
Billing Type	Invoice
Billing Address	The University of Tokyo Rm. 334, Eng. Bldg. 4 7-3-1, Hongo Bunkyo-ku, Japan 113-8656 Attn: The University of Tokyo
Total	0 JPY

Terms and Conditions**TERMS AND CONDITIONS FOR REUSE OF IEEE MATERIAL SELECTED FOR LICENSING (THE "LICENSED MATERIAL") BASED ON "TYPE OF USE" AND "FORMAT" SELECTED FOR LICENSING BY USER**

By clicking "accept" in connection with completing this licensing transaction, you, as "User" do agree that the following terms and conditions apply to the use of the material you selected for licensing (the "Licensed Material"), along with the Billing and Payment terms and conditions established by Copyright Clearance Center, Inc. ("CCC"), at the time that you opened your RightsLink account and that are available at any time at <http://myaccount.copyright.com>.

Grant of Limited License

IEEE hereby grants to you a non-exclusive, non-transferable worldwide license to use the Licensed Material in the "TYPE OF USE" and "FORMAT" that you outlined in the RightsLink form in connection with this transaction, and as outlined in accordance with the terms and conditions of this Agreement. This license does not include any photography, illustrations or advertisements that may appear in connection with the Licensed Material and does not extend to any revision or subsequent edition in which the Licensed Material may appear.

Types of Use

Complete terms and conditions and "TYPES OF USE" can be found in the License Agreement that will be available to you during the online order process. Certain terms of use in some IEEE licenses may take precedence over and supersede certain rights granted through RightsLink services. IEEE also reserves the right to restrict the types and total number of items that may be reused in any type of publication or medium. For additional information on the types of use available by IEEE and through RightsLink, please refer to http://www.ieee.org/publications_standards/publications/rights/rightslink_usetypes.html.

Authorized Use

The license granted is granted for a one-time use for REPUBLICATION IN THE "TYPE OF USE" and "FORMAT" that you outlined in the RightsLink form in connection with this transaction, to be completed within one (1) year from the date upon which this license is effective, with a maximum distribution equal to the number that you identified in the RightsLink form in connection with this transaction.

Restrictions on Use

All uses not specifically authorized in this license and specified in the options for reusing IEEE Licensed Material available through the RightsLink service are prohibited, including (i) altering or modifying the Licensed Material in any manner, translating the Licensed Material into another language or creating any derivative work based on the Licensed Material; (ii) storing or archiving the Licensed Material in any electronic medium or in any form now invented or devised in the future, except where permission is granted to do so. For additional information on the types of use available by IEEE and through RightsLink, please refer to

http://www.ieee.org/publications_standards/publications/rights/rightslink_usetypes.html .

If the Licensed Material is altered or modified in any manner, it must be within the scope of the license granted and it must not alter the meaning of the Licensed Material or in any way reflect negatively on the IEEE or any writer of the Licensed Material.

Any use of the Licensed Material in any way that would be considered libelous, defamatory, abusive or obscene, in violation of any applicable law or the proprietary rights of a third party and or used in connection with the advertising or promotion of any product or service is also prohibited.

You agree to use your best efforts to prevent unauthorized use of the Licensed Material.

License Effective Only Upon Payment and Author Approval

The license granted to you is effective only upon (i) receipt of full payment from you as provided in CCC's Billing and Payment terms and conditions and (ii) your having obtained the author's approval of your proposed use of the Licensed Material as described here.

IEEE Intellectual Property Rights

You agree that IEEE is the owner of all right, title and interest in the Licensed Material and/or has the right to license the Licensed Material, including all copyright rights and other intellectual property rights under United States and international law.

Termination

In the event that you breach any of these terms and conditions or any of CCC's Billing and Payment terms and conditions, the license granted herein shall be terminated immediately. Any use of the Licensed Material after termination, as well as any use of the Licensed Material beyond the scope of these terms and conditions, may constitute copyright infringement and IEEE reserves the right to take any and all action to protect its rights in the Licensed Material.

Copyright Notice

You must include the following copyright and permission notice (WITH DETAILS FILLED IN BY YOU) in connection with the Authorized Use of the Licensed Material:

© [Year] IEEE. Reprinted, with permission, from [complete publication information].

Warranty and Indemnity

You warrant that you have all rights necessary to enter into this agreement and hereby indemnify and agree to hold harmless IEEE and CCC, and their respective officers, directors, employees and agents, from and against any and all claims arising out of your use of the Licensed Material other than as specifically authorized pursuant to this license.

Limited Warranty and Limitation of Liability

THE RIGHT TO USE THE LICENSED MATERIAL IS GRANTED ON AN "AS IS" BASIS AND IEEE MAKES NO WARRANTY, EXPRESS OR IMPLIED WITH RESPECT TO THE LICENSED MATERIAL, INCLUDING ALL WARRANTIES OF QUALITY, ACCURACY AND/OR FITNESS FOR A PARTICULAR PURPOSE, AND IEEE SHALL NOT BE LIABLE UNDER ANY CIRCUMSTANCES FOR ANY LOSSES RESULTING FROM YOUR RELIANCE ON OR USE OF ANY INFORMATION CONTAINED IN THE LICENSED MATERIAL.

No Transfer or Assignment of License

This license is personal to you and may not be sublicensed, assigned, or transferred by you to any other person without IEEE's written permission.

Objection to Contrary Terms

IEEE hereby objects to any terms contained in any purchase order, acknowledgment, check endorsement or other writing prepared by you, which terms are inconsistent with these terms and conditions or CCC's Billing and Payment terms and conditions. These terms and conditions, together with CCC's Billing and Payment terms and conditions (which are incorporated herein), comprise the entire agreement between you and IEEE concerning this licensing transaction. In the event of any conflict between your obligations established by these terms and conditions and those established by CCC's Billing and Payment terms and conditions, these terms and conditions shall control.

Payment Terms

If you would like to pay for this license now, please remit this license along with your payment made payable to "COPYRIGHT CLEARANCE CENTER" otherwise you will be invoiced within 48 hours of the license date. Payment should be in the form of a check or money order referencing your account number and this invoice number. Payments should be sent to the address noted below:

Copyright Clearance Center
29118 Network Place
Chicago, IL 60673-1291

Once you receive your invoice for this order, you may pay by credit card. Additional information is provided to users at the time their credit card order is placed.

For suggestions or comments regarding this order, contact RightsLink Customer Support: customercare@copyright.com or +1-855-239-3415 (toll free in the US) or +1-978-646-2777.

Comments and Questions for IEEE

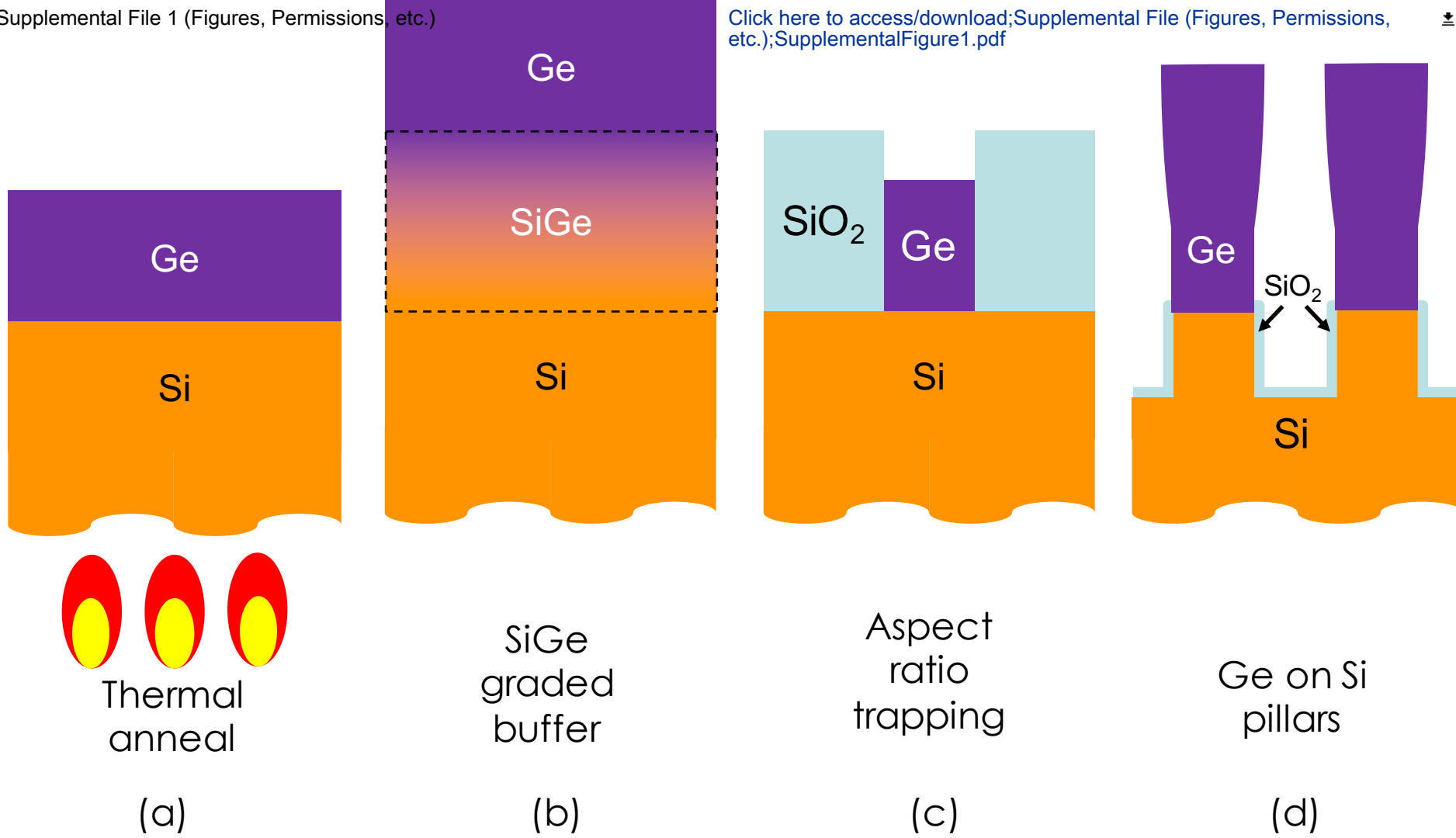
All comments and/or questions related to RightsLink permission services or comments and questions regarding IEEE licensing policies should be sent to discoverservices@ieee.org. Users may also call Author Support & Content Discovery staff at 732.562.3965.

A copy of both the license and these terms should be retained for your files.

Other Terms and Conditions:

Updated 12/2011 nbd-IEEE

Questions? customercare@copyright.com or +1-855-239-3415 (toll free in the US) or +1-978-646-2777.





Click here to access/download
Supplemental Coding Files
SupplementalVideo1.mp4

